
ESTIMATING RATE OF CHANGE FOR NONLINEAR TRAJECTORIES IN THE FRAMEWORK OF INDIVIDUAL MEASUREMENT OCCASIONS: A NEW PERSPECTIVE OF GROWTH CURVES

Jin Liu *

Department of Biostatistics
Virginia Commonwealth University

May 17, 2022

ABSTRACT

Researchers are interested in examining between-individual differences in within-individual changes. If the process under investigation is tracked for a long time, its trajectory may show a certain degree of nonlinearity, so the rate-of-change is not constant. A fundamental goal of modeling such nonlinear processes is to estimate model parameters that reflect meaningful aspects of change, including the rate-of-change and other parameters that shed light on substantive hypotheses. However, if the measurement occasion is unstructured, existing models cannot simultaneously estimate these two types of parameters. This article has three goals. First, we view the change over time as the area under the curve (AUC) of the rate-of-change versus time ($r - t$) graph. Second, with the instantaneous rate-of-change midway through a time interval to approximate the average rate of change during that interval, we propose a new specification to describe longitudinal processes. In addition to obtaining the individual rate-of-change and other parameters related to specific research questions, the new specification allows for unequally-space study waves and individual measurement occasions around each wave. Third, we derive the model-based change-from-baseline, a common measure to evaluate change over time. We evaluate the proposed specification through a simulation study and a real-world data analysis. We also provide *OpenMx* and *Mplus 8* code for each model with the novel specification.

Keywords Longitudinal Processes with Nonlinear Trajectories · Area under the Curve · Latent Growth Curve Models · Latent Change Score Models · Individual Measurement Occasions

1 Introduction

Researchers have widely employed longitudinal models to assess between-individual differences in within-individual changes in multiple fields, including psychology, education, biomedicine, and behavioral sciences. The linear curve is the most commonly used function when fitting longitudinal records due to its simplicity and interpretability. An individual linear trajectory has two free coefficients: the intercept and the constant linear slope, representing the outcome of interest at a specific time point (usually at the first study wave) and the rate-of-change over the study duration, respectively. The intercept and the slope are allowed to vary from person to person in commonly used longitudinal modeling frameworks, such as mixed-effect and latent growth curve models. The investigation of individual differences in the intercept and slope is one primary interest in exploring longitudinal records Biesanz et al. (2004); Zhang et al. (2012); Grimm et al. (2013b).

However, if the process under examination is followed for a long time, the trajectory of the longitudinal process may show a certain degree of nonlinearity to time. Multiple existing studies have discussed the rate-of-change of nonlinear trajectory. For example, (Kelley and Maxwell, 2008) delineated the average rate of change (ARC) as the change in the

*CONTACT Jin Liu Email: Veronica.Liu0206@gmail.com

outcome measurement divided by the change in time during a specific time interval and demonstrated that the ARC and the slope from the straight-line change model are not equal to each other in general. In addition, (Kelley, 2009) extended such descriptions and demonstrations to the continuous-time models. For those nonlinear trajectories, it is a challenge to directly estimate the rate-of-change at the individual level because it is usually a combination of multiple coefficients. For example, the rate-of-change of the quadratic function (i.e., $y = a \times t^2 + b \times t$), a commonly used nonlinear curve, consists of a linear slope (i.e., b) and a quadratic slope (i.e., $2 \times a \times t$). The latter changes over the study duration, so does the rate-of-change.

Another challenge of longitudinal data analysis is related to the measurement occasion. On the one hand, researchers may not record a longitudinal outcome at a constant frequency, resulting in unequal intervals between study waves. For example, in some popular longitudinal studies, such as the Early Childhood Longitudinal Research Project, assessments are collected more frequently in the early stage Lê et al. (2011). On the other hand, the measurement times of each research wave Finkel et al. (2003); Mehta and West (2000) may be different. If the time is accurate, such unstructured measurement occasions will appear. For example, if we evaluate students' academic performance for each grade/semester, we have a regular measurement schedule, but if we evaluate their academic performance based on their actual age, the measurement time is individually different (Grimm et al., 2016, Chapter 4). Researchers have performed simulation studies and shown that the neglect of individual differences in measurement occasions may lead to inadmissible estimates, such as overestimated intra-individual variation and underestimated inter-individual differences Blozis and Cho (2008); Coulombe et al. (2015).

Theoretical and empirical researchers have proposed and utilized various frameworks to model trajectories, including mixed-effects (or multi-level) modeling frameworks (e.g., (Harville, 1977; Lindstrom and Bates, 1990; Laird and Ware, 1982; Hedeker and Gibbons, 2006; Pinheiro, 1994; Vonesh and Carter, 1992; Bryk and Raudenbush, 1987)) and latent growth curve modeling (LGCM) framework (e.g., (Grimm et al., 2016; Ram and Grimm, 2007; Duncan et al., 2000, 2013; Bollen and Curran, 2005)). These two modeling frameworks are mathematically equivalent in almost all cases Bauer (2003); Curran (2003), except that the approximation methods to fit the models without closed-form of the likelihood function in the two frameworks are different Liu et al. (2021). Therefore, in most cases, two frameworks can provide the same results. This article focuses on the LGCM, which is one type of model in the structural equation modeling (SEM) framework.

The mixed-effect model and LGCM can be used to model linear or nonlinear trajectories. However, we cannot directly estimate the rate-of-change in their original forms, except for the linear one Zhang et al. (2012), or more broadly, the model with a single between-individual coefficient affecting time Grimm et al. (2013c). Fortunately, recent studies, for example, (Zhang et al., 2012; Grimm et al., 2013c.a) have shown the use of a latent change score model (LCSM) to examine the rate-of-change by taking the first-order derivative of the corresponding LGCM with respect to time t . The LCSM allows for an explicit estimation of the mean and variance of the rate-of-change over time and then a direct examination of the individual differences in the rate-of-change and its relationship with covariates. However, the LCSM was proposed to assume that the time is discrete and, therefore, these measurements are equally-spaced. Though some recent studies, for example, (Grimm and Jacobucci, 2018), have demonstrated that the time can also be continuous and constructed the LCSMs with individually measurement occasions with the *NLMIXED* procedure in *SAS* or using Bayesian modeling tools such as *JAGS* or *WinBUGS*, there are still unsolved challenges, which we will introduce later.

In this study, we extend the existing LCSM to directly estimate the rate-of-change for nonparametric and nonlinear parametric growth trajectories in the framework of individual measurement occasions. Specifically, we regard the growth over time as the area under the curve (AUC) of the rate-of-change versus time (r - t) graph and propose a novel specification to describe the longitudinal process. The new specification is supposed to provide a more accurate estimate of a growth coefficient than the existing LCSM specification computationally efficiently. In addition, with the novel specification, it is easier to estimate change-from-baseline (i.e., the change in measurements from the start of a study), a common metric to evaluate growth over time in a longitudinal study.

The rest of this article is organized as follows. First, we present nonparametric and three commonly used nonlinear parametric functions (including quadratic, negative exponential, and Jeness-Bayley curves) in the LGCM and LCSM frameworks. Next, we describe the model specification and estimation of each extended LCSM with the above four functions. In the following section, we show the design of a Monte Carlo simulation to evaluate the novel specification. Specifically, we present performance metrics, including the relative bias, the empirical standard error (SE), the relative root-mean-squared-error (RMSE), and the empirical coverage probability (CP) for a nominal 95% confidence interval of parameters of interest. We also compare each LCSM with the novel specification with the corresponding LGCM. In the Application section, we analyze a real-world dataset to demonstrate how to fit and interpret the LGCM and LCSM. Finally, we discuss practical considerations, methodological considerations, and future directions.

1.1 Introduction of Latent Growth Curve Modeling Framework

The LGCM is a modeling framework in the SEM family, focusing on analyzing absolute measurements. This section briefly introduces this modeling framework with an overview of commonly used functions, including quadratic, exponential, Jenss-Bayley, and nonparametric functions. In the SEM terminology, a typical growth curve model is fit as a common factor model with a mean structure Tucker (1958); Rao (1958); Meredith and Tisak (1990), and the factors in a LGCM are often called growth factors since they determine the shape of growth curves. A LGCM can be expressed as $\mathbf{y}_i = \mathbf{\Lambda} \times \boldsymbol{\eta}_i + \boldsymbol{\epsilon}_i$, where \mathbf{y}_i is a $J \times 1$ vector of the repeated measures of the i^{th} individual (in which J is the number of measurements), $\boldsymbol{\eta}_i$ is a $k \times 1$ vector of latent growth factors for individual i (where k is the number of growth factors), and $\mathbf{\Lambda}$ is a $J \times k$ matrix of the corresponding factor loadings. Additionally, $\boldsymbol{\epsilon}_i$ is a $J \times 1$ vector of residuals of individual i . Table 1 provides the LGCM with multiple commonly used parametric functions and a nonparametric function.

=====
 Insert Table 1 about here
 =====

The LGCM with the quadratic function (see Figure 1b), which is the simplest nonlinear polynomial LGCM, has three growth factors to indicate the initial status (η_{0i}), the linear component of change (η_{1i}), and the quadratic component of change (η_{2i}), respectively. The mean values of these growth factors are of primary interest for the investigation of the model, so is the variance-covariance matrix of these growth factors, which allows for individual differences in these growth coefficients and then growth curves.

=====
 Insert Figure 1 about here
 =====

The LGCM with the negative exponential function (see Figure 1c) can be expressed as such in Table 1, where η_{0i} and η_{1i} are growth factors that represent the initial status and the amount of change from the initial state to the asymptotic level. An additional coefficient b represents the logarithmic ratio of rate-of-change at t_j to that at t_{j-1} . According to (Browne and du Toit, 1991; Preacher and Hancock, 2012, 2015), the coefficient b can also be at the individual level (i.e., a growth factor) through the Taylor series expansion so that the target function is a linear combination of all growth factors (i.e., η_{0i} , η_{1i} and b).

The Jenss-Bayley function (see Figure 1d and its equation in Table 1) is a negative-accelerated exponential component that approaches a linear asymptote with a positive slope². There are three growth factors in the Jenss-Bayley LGCM to indicate the initial status (η_{0i}), the slope of the linear asymptote (η_{1i}), and the vertical distance between the initial status and the intercept of the linear asymptote (η_{2i}), respectively. Furthermore, we have a coefficient c , which represents the logarithmic ratio of the growth acceleration at t_j to that at t_{j-1} . Like the coefficient b in the negative exponential function, c can also be an additional growth factor through the Taylor series expansion.

One advantage of a parametric LGCM is that its parameters are potentially related to theory, allowing us to formulate hypotheses more easily. For example, the quadratic component of the change in the quadratic function is usually interpreted as how quickly the change in rate-of-change is (i.e., the acceleration). In addition, researchers often view the asymptotic level in the negative exponential function as the individual limits to reflect the individual's capacity. However, we may need more coefficients (e.g., a higher degree of the polynomial function) or nonlinear growth factors (e.g., an individual ratio of the growth acceleration in the Jenss-Bayley function) to describe more complex nonlinear change patterns, which may lead to a non-parsimonious model or one that involves an approximation process.

An alternative is to consider nonparametric functions. The LGCM with a nonparametric function is usually referred to as a latent basis growth model (LBGM) Grimm et al. (2011), or a shape-factor or free-loading model Bollen and Curran (2006); McArdle (1986). It is a versatile tool to explore nonlinear trajectories: it does not require any function to describe the underlying change patterns, its estimation process is expeditious, and its coefficients are straightforward to interpret. In the LBGM, there are two growth factors (i.e., $k = 2$), a factor indicating the initial status (η_{0i}) and a shape factor (η_{1i}). For model identification considerations, we need to fix intercept factor loadings and any two loadings from the shape factor³. There are multiple ways to scale and specify the shape factor of a LBGM. For example, if we scale the shape factor as the change during the first time period (i.e., the time interval between the first and second

²If the slope is zero, this growth curve reduces to a negative exponential function.

³The loading from the shape factor to the first measurement is zero since the intercept is sufficient to indicate the initial status, and thus, we only need to fix one loading among others.

measurements), the unknown loading, λ_j ($j = 2, 3, \dots, J - 1$), represents the quotient of the change-from-baseline at the $(j + 1)^{th}$ measurement occasion to the shape factor.

As stated earlier, longitudinal records may not be taken at a constant frequency, and individuals may have different measurement time points for each study wave. In the LGCM framework, one possible solution to the challenge of individual measurement occasions⁴ is the definition variable approach Sterba (2014); Preacher and Hancock (2015); Liu et al. (2021). The ‘definition variable’ is defined as an observed variable that adjusts model coefficients to individual-specific values Mehta and West (2000); Mehta and Neale (2005). In the LGCM, these individual-specific values are individually different time points. Details of specification and estimation of the LGCM with individual measurement times are available in earlier studies such as (Sterba, 2014; Preacher and Hancock, 2015; Liu et al., 2021).

1.2 Introduction of Latent Change Score Modeling Framework

As discussed above, while LGCMs are available with multiple parametric functions and the nonparametric function (i.e., the latent basis growth model) and can be fit in the framework of individual measurement occasions, their focus is to characterize **the time-dependent state**. However, one primary research interest for longitudinal processes, especially for those nonlinear longitudinal trajectories, is to estimate the rate-of-change and the cumulative value of the rate-of-change over time. In this scenario, LGCMs may not be very helpful. Therefore, we introduce another modeling framework, LCSMs, which emphasizes **the time-dependent change** in this section with an overview of the four functional forms as above.

LCSMs, which are also referred to as latent difference score models McArdle (2001); McArdle and Hamagami (2001); McArdle (2009), were developed to integrate difference equations into the SEM framework. In the LCSM, the difference scores are sequential temporal states of a longitudinal outcome. Specification of the LCSM starts from the idea of classical test theory: for each individual, the observed score at a specific occasion can be decomposed into a latent true score and a residual⁵

$$y_{ij} = ly_{ij} + \epsilon_{ij},$$

in which y_{ij} , ly_{ij} and ϵ_{ij} are the observed score, the latent true score, and the residual of individual i at time j , respectively. The true score at time j (i.e., ly_{ij}) can be further expressed as a linear combination of the true score at the prior time point $j - 1$ (i.e., $ly_{i(j-1)}$) and the latent change score from time $j - 1$ to time j (i.e., Δy_{ij})

$$ly_{ij} = ly_{i(j-1)} + \Delta y_{ij}.$$

The parameters of interest for a LCSM include (1) the mean and variance of the initial status, (2) the mean and variance of each latent change score, and (3) the residual variance. The estimated means and variances of the change scores allow for examining the within-individual changes in between-individual differences in the rate-of-change.

(McArdle, 2001) and (Grimm et al., 2016, Chapter 11) have shown that the LGCM with the nonparametric function (i.e., the LBGCM) can also be fit in the LCSM framework. They expressed a linear latent curve model in the LCSM framework in which the individual latent change score is a constant and scaled the score by time-varying basis coefficients. Therefore, a latent change score can be written as

$$\Delta y_{ij} = a_j \times \eta_{1i}, \quad (1)$$

where a_j is the time-varying basis coefficient of the constant factor η_{1i} at time j . Similar to the LBGCM in the LGCM framework, we can fix the basis coefficient of the first time period to 1 for model identification, so η_{1i} represents the slope of the first time period. In addition, (Zhang et al., 2012) and (Grimm et al., 2013b) have shown that a LGCM with a parametric function also has its corresponding LCSM. We provide the equation and plot of the rate-of-change for the nonparametric and each parametric LCSM in Table 2 and Figure 2, respectively. When estimating these parametric nonlinear LCSMs, the rate at t_j is employed to approximate the rate during the interval (t_{j-1}, t_j) in the existing specification. The coefficients in each parametric LCSM have the same interpretation as those in the corresponding LGCM. In addition to the parameters that contribute to the rate-of-change, we also need to estimate the mean and variance of the initial status when fitting a parametric LCSM.

⁴The time structure with unequal intervals and individual measurement occasions is also referred to as ‘continuous time’ Driver et al. (2017); Driver and Voelkle (2018). One difference between the models discussed in the article and the ‘continuous-time’ models is that the former can estimate growth parameters related to developmental theory and then is easier to make hypotheses, while the latter is used to analyze dynamic processes. So we do not use the term ‘continuous-time’ to avoid confusion.

⁵In classical test theory, the difference between the observed and true scores is usually referred to as a measurement error. However, ϵ_{ij} is usually called a residual or unique score at time j of individual i in the LGCM and LCSM literature. This manuscript then follows the convention in the LGCM and LCSM literature.

=====
 Insert Table 2 about here
 =====

=====
 Insert Figure 2 about here
 =====

We can use nonlinear LCSMs to simultaneously estimate individuals' rate-of-change over time and the parameters that are related to theory. Yet there are multiple assumptions for the model specification of the existing LCSM framework. First, it is usually assumed that the measurement times are equally-spaced. For example, in Equation 1, Δy_{ij} is the change from $t = j - 1$ to $t = j$, and $a_j \times \eta_{1i}$ is the slope of the time period between the two time points. They are mathematically equivalent if the slope is constant within the time interval and the interval between two measurement occasions is scaled. The constant slope assumption is established for the LBG⁶ (see Figure 2a), yet it is not satisfied in any parametric nonlinear LCSM (see Figures 2b-2d). Moreover, the assumption to ensure scaled time intervals is that the measurement times are equally-spaced, yet it is not always valid in the real world: researchers tend to record more frequently in the early stages of longitudinal studies, where changes are usually more rapid.

We use the rate-of-change versus time ($r - t$) graphs in Figure 2 to illustrate our point. According to the fundamental theorem of calculus, the AUC in a time interval of the $r - t$ graph is the amount of change in that interval. As shown in Figure 2a, the change score from $t = 0$ to $t = 1$ is 5, which is numerically equal to the slope of this period since the interval is scaled. However, this equivalence does not hold for the score from $t = 2$ to $t = 4$. We have a similar challenge for parametric nonlinear LCSMs. One recent study, (Grimm et al., 2016, Chapter 18), successfully solved the challenge of unequally-spaced measurement occasions by specifying a latent change score for each scaled period in the study duration. Suppose that we skip the measurements at $t = 3$. Using this method, we can define the latent change score from $t = 2$ to $t = 4$ as the sum of the change from $t = 2$ to $t = 3$ and that from $t = 3$ to $t = 4$. However, the model specification becomes complicated if the study duration is long or the scaled time interval is short.

Another challenge, specifically for a parametric nonlinear LCSM, is that the slope is not constant over a period. It may be valid to employ the rate-of-change at t_j to approximate the ARC during (t_{j-1}, t_j) as the existing LCSM framework. However, this approximation still results in bias: the change score is underestimated when the rate-of-change decreases, as the grey boxes in Figure 2c. The approximated change score from $t = 2$ to $t = 3$ and from $t = 4$ to $t = 6$ are enclosed by the solid and dashed box, respectively. Both are smaller than the true AUC of the corresponding time interval. Similarly, the change score is overrated if the rate-of-change increases.

Additionally, as stated before, some existing studies, for example, (Grimm and Jacobucci, 2018), proposed to specify a latent true score at an individual measurement occasion to obtain the score of each individual and built the model using SAS procedure *NLMIXED* and Bayesian modeling tools, such as *WinBUGs* and *JAGS*. However, the *NLMIXED* does not allow for specifying residual covariance that may lead to model misspecification and then bias, while those Bayesian tools require lots of computational resources⁷. To solve these challenges, we employ the instantaneous rate-of-change midway through an interval to approximate the ARC during the interval and propose a novel specification for the LCSM. This novel specification provides more accurate estimates and allows for the extension of the definition variable approach to fit the LCSM in the framework of individual measurement occasions.

2 Method

2.1 Model Specification of Nonparametric Latent Change Score Models

In this section, we present a new specification for the LBG⁶ in the LCSM framework. Following (McArdle, 2001) and (Grimm et al., 2016, Chapter 11), we view the LBG⁶ with J measures as a linear piecewise function with $J - 1$

⁶When defining a LBG⁶, it is reasonable to assume that the rate-of-change in each time-interval between two consecutive measurement occasions is constant for model identification. Therefore, the latent basis growth curve with J measurement occasions can be viewed as a linear piecewise function with $J - 1$ segments.

⁷In an example provided in (Grimm and Jacobucci, 2018), a JAGS model converged for all parameters after 50,000 samples and took over two hours.

segments. For the i^{th} individual, we specify the model as

$$y_{ij} = ly_{ij} + \epsilon_{ij}, \quad (2)$$

$$ly_{ij} = \begin{cases} \eta_{0i}, & \text{if } j = 1 \\ ly_{i(j-1)} + \Delta y_{ij}, & \text{if } j = 2, \dots, J \end{cases}, \quad (3)$$

$$\Delta y_{ij} = dy_{ij} \times (t_{ij} - t_{i(j-1)}) \quad (j = 2, \dots, J), \quad (4)$$

$$dy_{ij} = \eta_{1i} \times \gamma_{j-1} \quad (j = 2, \dots, J). \quad (5)$$

Equations 2 and 3 together define the basic setting of a LCSM, where y_{ij} , ly_{ij} , and ϵ_{ij} are the observed measurement, latent true score, and residual of the i^{th} individual at time j , respectively. At the first observation, the true score is the growth factor indicating the initial status (η_{0i}); otherwise, the true score at time j is a linear combination of the score at the prior time point $j - 1$ and the amount of true change from time $j - 1$ to j (Δy_{ij}). For each individual, as shown in Equation 4, we further express Δy_{ij} as the product of the time interval ($t_{ij} - t_{i(j-1)}$) and the slope (dy_{ij}) in that interval. As shown in Figure 2a, this production is the AUC of the $r - t$ graph from time $j - 1$ to j . Note that each time interval is not necessarily equal. The subscript i of t indicates that the measurement time is allowed to be individually different, so is the time interval. With the assumption that the residuals are time-independent, we then scale the shape factor (η_{1i}) to the slope in the first time interval and express the slope from $j - 1$ to j as the product of η_{1i} and the relative rate in that interval⁸ (γ_{j-1}) as Equation 5. We provide a path diagram of the LBGGM with six measurements using the novel specification in Figure 3a, where we use the diamond shape to denote the definition variables Mehta and Neale (2005); Sterba (2014) and illustrate the heterogeneity of the time intervals.

=====
Insert Figure 3 about here
=====

The model defined in Equations 2-5 can also be expressed in a matrix form

$$\mathbf{y}_i = \mathbf{\Lambda}_i \times \boldsymbol{\eta}_i + \boldsymbol{\epsilon}_i, \quad (6)$$

where \mathbf{y}_i is a $J \times 1$ vector of the repeated measurements of the i^{th} individual (in which J is the number of measures), $\boldsymbol{\eta}_i$ is a 2×1 vector of growth factors of which the first element is the initial status and the second element is the slope in the first time interval, and $\mathbf{\Lambda}_i$ is a $J \times 2$ matrix of the corresponding factor loadings

$$\mathbf{\Lambda}_i = \begin{pmatrix} 1 & 0 \\ 1 & \gamma_1 \times (t_{i2} - t_{i1}) \\ 1 & \sum_{j=2}^3 \gamma_{j-1} \times (t_{ij} - t_{i(j-1)}) \\ \dots & \dots \\ 1 & \sum_{j=2}^J \gamma_{j-1} \times (t_{ij} - t_{i(j-1)}) \end{pmatrix}. \quad (7)$$

The subscript i in $\mathbf{\Lambda}_i$ indicates that the model is built in the framework of individual measurement occasions. Similar to LGCMs, the first column of $\mathbf{\Lambda}_i$ is the factor loadings of the intercept, so all loadings are 1. The j^{th} element in the second column is the cumulative value of the relative rate⁹ over time up to time j , so the product of it and η_{1i} represents the change from the initial status, which is also the value of AUC of $r - t$ graph from the start to time j . Additionally, $\boldsymbol{\epsilon}_i$ is a $J \times 1$ vector of residuals of the i^{th} individual. The growth factors $\boldsymbol{\eta}_i$ can be further expressed as

$$\boldsymbol{\eta}_i = \boldsymbol{\mu}_\eta + \boldsymbol{\zeta}_i, \quad (8)$$

in which $\boldsymbol{\mu}_\eta$ is the mean vector of the growth factors, and $\boldsymbol{\zeta}_i$ is the vector of deviations of individual i from the corresponding mean values of growth factors.

2.2 Model Specification of Parametric Latent Change Score Models

This section presents the new specification for nonlinear parametric LCSMs. The specification of a parametric model is tricky since the rate-of-change in each time interval is not constant, as shown in Figures 2b-2d. To solve this challenge, we propose to utilize the instantaneous slope midway of the time interval (t_{j-1}, t_j) to approximate the ARC in that interval. We illustrate this idea using grey boxes in Figure 2d. For example, for the change score from $t = 2$ to $t = 3$, we use the instantaneous slope at $t = 2.5$ to approximate the ARC, and therefore, the approximated latent change score

⁸In this current study, we define the relative rate to η_{1i} as the absolute rate-of-change divided by η_{1i} .

⁹Note that the relative rate from t_{i1} to t_{i2} is fixed as 1 (i.e., $\gamma_1 = 1$) for identification consideration.

is the area in the solid box. Similarly, the approximated change from $t = 4$ to $t = 6$ is the area in the dashed box, with the ARC set as the instantaneous slope at $t = 5$.

When specifying the nonlinear parametric LCSMs, we still need to set up the basic LCSM as Equations 2 and 3, and then we need to redefine the latent change score of each interval as the product of the instantaneous slope in the middle of that interval and the corresponding interval length

$$\Delta y_{ij} \approx dy_{ij_mid} \times (t_{ij} - t_{i(j-1)}), \quad (9)$$

in which dy_{ij_mid} is the slope at the midpoint from $j - 1$ to j . For the i^{th} individual, the instantaneous slope of quadratic, exponential and Jents-Bayley curves can be written as

- Quadratic Function:

$$\begin{aligned} dy_{ij_mid} &= \frac{d}{dt} (\eta_{0i} + \eta_{1i} \times t + \eta_{2i} \times t^2 + \epsilon_{ij})|_{t=t_{ij_mid}} \\ &= \eta_{1i} + 2 \times \eta_{2i} \times t_{ij_mid}, \end{aligned} \quad (10)$$

- Negative Exponential Function:

$$\begin{aligned} dy_{ij_mid} &= \frac{d}{dt} (\eta_{0i} + \eta_{1i} \times (1 - \exp(-b \times t)) + \epsilon_{ij})|_{t=t_{ij_mid}} \\ &= b \times \eta_{1i} \times \exp(-b \times t_{ij_mid}), \end{aligned} \quad (11)$$

- Jents-Bayley function:

$$\begin{aligned} dy_{ij_mid} &= \frac{d}{dt} (\eta_{0i} + \eta_{1i} \times t + \eta_{2i} \times (\exp(c \times t) - 1) + \epsilon_j)|_{t=t_{ij_mid}} \\ &= \eta_{1i} + c \times \eta_{2i} \times \exp(c \times t_{ij_mid}). \end{aligned} \quad (12)$$

With this definition, Δy_{ij} defined in Equation 9 is an approximated value of the AUC of a parametric $r - t$ graph (i.e., an approximated value of the change) from time $j - 1$ to j . Each coefficient in Equations 10, 11, and 12 is interpreted as the corresponding element introduced in Table 1. Similar to the nonparametric LCSM, these parametric nonlinear LCSMs can be expressed in the matrix form as Equations 6 and 8. For the quadratic, negative exponential, and Jents-Bayley models, $\boldsymbol{\eta}_i$ is a 3×1 , 2×1 , and 3×1 vector of growth factors, respectively, and their corresponding factor loading matrices are

- Quadratic Function:

$$\boldsymbol{\Lambda}_i = \begin{pmatrix} 1 & 0 & 0 \\ 1 & (t_{i2} - t_{i1}) & 2 \times t_{i2_mid} \times (t_{i2} - t_{i1}) \\ 1 & \sum_{j=2}^3 (t_{ij} - t_{i(j-1)}) & 2 \times \sum_{j=2}^3 t_{ij_mid} \times (t_{ij} - t_{i(j-1)}) \\ \dots & \dots & \dots \\ 1 & \sum_{j=2}^J (t_{ij} - t_{i(j-1)}) & 2 \times \sum_{j=2}^J t_{ij_mid} \times (t_{ij} - t_{i(j-1)}) \end{pmatrix}, \quad (13)$$

- Negative Exponential Function:

$$\boldsymbol{\Lambda}_i = \begin{pmatrix} 1 & 0 \\ 1 & b \times \exp(-b \times t_{i2_mid}) \times (t_{i2} - t_{i1}) \\ 1 & b \times \sum_{j=2}^3 \exp(-b \times t_{ij_mid}) \times (t_{ij} - t_{i(j-1)}) \\ \dots & \dots \\ 1 & b \times \sum_{j=2}^J \exp(-b \times t_{ij_mid}) \times (t_{ij} - t_{i(j-1)}) \end{pmatrix}, \quad (14)$$

- Jeness-Bayley function:

$$\mathbf{\Lambda}_i = \begin{pmatrix} 1 & 0 & 0 \\ 1 & (t_{i2} - t_{i1}) & c \times \exp(c \times t_{i2_mid}) \times (t_{i2} - t_{i1}) \\ 1 & \sum_{j=2}^3 (t_{ij} - t_{i(j-1)}) & c \times \sum_{j=2}^3 \exp(c \times t_{ij_mid}) \times (t_{ij} - t_{i(j-1)}) \\ \dots & \dots & \dots \\ 1 & \sum_{j=2}^J (t_{ij} - t_{i(j-1)}) & c \times \sum_{j=2}^J \exp(c \times t_{ij_mid}) \times (t_{ij} - t_{i(j-1)}) \end{pmatrix}. \quad (15)$$

Similar to the first column of $\mathbf{\Lambda}_i$ in Equation 7, the first column of $\mathbf{\Lambda}_i$ in Equations 13-15 are the factor loadings of the intercept, but they are for the quadratic, negative exponential, and Jeness-Bayley functions, respectively. In addition, the second and third columns of $\mathbf{\Lambda}_i$ in Equation 13 represent the cumulative value of the linear slope (i.e., 1) and that of the quadratic slope (i.e., $2 \times t_{ij_mid}$) over time, respectively. Similarly, the second column of $\mathbf{\Lambda}_i$ in Equation 14 is the cumulative value of the negative exponential slope (i.e., $b \times e^{-b \times t_{ij_mid}}$) over time, while the second and third columns of $\mathbf{\Lambda}_i$ in Equation 15 are the cumulative value of the linear asymptote slope (i.e., 1) and that of the exponential slope (i.e., $c \times e^{c \times t_{ij_mid}}$) over time, respectively. With such specifications, the j^{th} element of the product of the grey part of each $\mathbf{\Lambda}_i$ and the corresponding growth factor(s) is interpreted as the change-from-baseline at time j for the corresponding parametric LCSM, which is also an approximate value of AUC of $r - t$ graph from the start to time j . We provide path diagram for these parametric LCSMs (six measurements) using the novel specification in Figures 3b-3d.

2.3 Model Estimation

To simplify estimation, we make two assumptions. First, we assume that the growth factors in each LCSM are normally distributed; that is, $\zeta_i \sim \text{MVN}(\mathbf{0}, \mathbf{\Psi}_\eta)$, where $\mathbf{\Psi}_\eta$ is a 2×2 , 3×3 , 2×2 , and 3×3 variance-covariance matrix of the growth factors of the nonparametric, quadratic, negative exponential, and Jeness-Bayley LCSM, respectively. We also assume that residuals are independently and identically normally distributed, that is, for the i^{th} individual, $\epsilon_i \sim \text{MVN}(\mathbf{0}, \theta_\epsilon \mathbf{I})$, where \mathbf{I} is a $J \times J$ identity matrix. Therefore, for the individual i , the expected mean vector and the variance-covariance structure of the repeated measurements \mathbf{y}_i of a LCSM specified in Equations 6 and 8 are expressed as

$$\boldsymbol{\mu}_i = \mathbf{\Lambda}_i \boldsymbol{\mu}_\eta$$

and

$$\boldsymbol{\Sigma}_i = \mathbf{\Lambda}_i \mathbf{\Psi}_\eta \mathbf{\Lambda}_i^T + \theta_\epsilon \mathbf{I}.$$

The parameters of each LCSM given in Equations 6 and 8 include the mean vector and variance-covariance matrix of the growth factors, and the residual variance. In addition, we need to estimate the relative rate of each time interval for the nonparametric LCSM (i.e., γ_j), while we have to estimate the coefficient b for the negative exponential LCSM and coefficient c for the Jeness-Bayley LCSM. The parameters of each LCSM presented above are detailed below

- Nonparametric Function (i.e., LBGGM):

$$\begin{aligned} \Theta_{\text{LBGM}} &= \{\boldsymbol{\mu}_\eta, \mathbf{\Psi}_\eta, \gamma_2, \dots, \gamma_{J-1}, \theta_\epsilon\} \\ &= \{\mu_{\eta_0}, \mu_{\eta_1}, \psi_{00}, \psi_{01}, \psi_{11}, \gamma_2, \dots, \gamma_{J-1}, \theta_\epsilon\} \end{aligned}$$

- Quadratic Function:

$$\begin{aligned} \Theta_{\text{QUAD}} &= \{\boldsymbol{\mu}_\eta, \mathbf{\Psi}_\eta, \theta_\epsilon\} \\ &= \{\mu_{\eta_0}, \mu_{\eta_1}, \mu_{\eta_2}, \psi_{00}, \psi_{01}, \psi_{02}, \psi_{11}, \psi_{12}, \psi_{22}, \theta_\epsilon\} \end{aligned}$$

- Negative Exponential Function:

$$\begin{aligned} \Theta_{\text{EXP}} &= \{\boldsymbol{\mu}_\eta, \mathbf{\Psi}_\eta, b, \theta_\epsilon\} \\ &= \{\mu_{\eta_0}, \mu_{\eta_1}, \psi_{00}, \psi_{01}, \psi_{11}, b, \theta_\epsilon\} \end{aligned}$$

- Jeness-Bayley function:

$$\begin{aligned}\Theta_{\text{JB}} &= \{\boldsymbol{\mu}_\eta, \boldsymbol{\Psi}_\eta, c, \theta_\epsilon\} \\ &= \{\mu_{\eta_0}, \mu_{\eta_1}, \mu_{\eta_2}, \psi_{00}, \psi_{01}, \psi_{02}, \psi_{11}, \psi_{12}, \psi_{22}, c, \theta_\epsilon\}\end{aligned}$$

We use the full information maximum likelihood (FIML) technique to estimate each proposed LCSM to account for the heterogeneity of individual contributions to the likelihood. The log-likelihood function of each individual and the overall sample are

$$\log \text{lik}_i(\Theta_{\text{LBGM/QUAD/EXP/IB}} | \mathbf{y}_i) = C - \frac{1}{2} \ln |\boldsymbol{\Sigma}_i| - \frac{1}{2} (\mathbf{y}_i - \boldsymbol{\mu}_i)^T \boldsymbol{\Sigma}_i^{-1} (\mathbf{y}_i - \boldsymbol{\mu}_i),$$

and

$$\log \text{lik}(\Theta_{\text{LBGM/QUAD/EXP/IB}}) = \sum_{i=1}^n \log \text{lik}_i(\Theta_{\text{LBGM/QUAD/EXP/IB}} | \mathbf{y}_i),$$

respectively, in which C is a constant, n is the number of individuals, $\boldsymbol{\mu}_i$ and $\boldsymbol{\Sigma}_i$ are the mean vector and the variance-covariance matrix of the longitudinal outcome \mathbf{y}_i . We use the R package *OpenMx* with the optimizer CSOLNP Neale et al. (2016); Pritikin et al. (2015); Hunter (2018); Boker et al. (2020) to build the proposed models. We provide *OpenMx* code in the online appendix (https://github.com/Veronica0206/Extension_projects) (code will be uploaded upon acceptance) to demonstrate how to employ the proposed novel specification. The proposed LCSMs with the novel specification can also be fit using other SEM software such as *Mplus* 8. We also provide the corresponding code on the Github website for researchers who are interested in using it.

In addition to the growth factors, the rate-of-change (i.e., dy_{ij} in the LBGM or dy_{ij_mid} in the parametric nonlinear LCSM) and true score (i.e., ly_{ij}) at each time point are also latent variables in the LCSM framework, as shown in Figure 3, but the means and variances of them are not free parameters. We can derive the mean and variance of dy_{ij} (dy_{ij_mid}) from Equation 5 (Equations 10-12) by using the Delta Method Lehmann and Casella (1998, Chapter 1). The detailed derivation is provided in Appendix Appendix A. Additional research interest is to estimate the amount of change-from-baseline, which is a common metric to evaluate the effect of an intervention. It is straightforward to estimate these values with the proposed model specification since each element of the product of the grey part of each Λ_i in Equations 7, 13, 14, and 15 and the corresponding growth factor(s) is the amount of change-from-baseline at each post-baseline time point. In practice, we can specify the expression for this type of derived parameters in the function *mxAlgebra()*, and then evaluate the corresponding point estimate and standard error by using function *mxEval()* and *mxSE()*, respectively. In practice, it may also be of interest to calculate latent variables at the individual level, which can be realized by the *OpenMx* function *mxFactorScores()* Neale et al. (2016); Pritikin et al. (2015); Hunter (2018); Boker et al. (2020); Estabrook and Neale (2013). We provide the corresponding code for these possible applications in the GitHub website.

3 Model Evaluation

We perform a Monte Carlo simulation study to evaluate the proposed model specification with two objectives. The first objective is to examine the four models with the novel specification introduced in the Method section through performance metrics, including the relative bias, empirical SE, relative RMSE, and empirical CP for a nominal 95% confidence interval of each parameter. In Table 3, we provide the definitions and estimates of these four performance measures. The second objective is to evaluate how the approximated value of the AUC (i.e., the latent change score) in each time interval affects the performance metrics of each nonlinear parametric LCSM. To this end, we generate LGCM-implied data structures for each parametric model, build up the corresponding LGCM and LCSM, and compare the four performance metrics.

=====
 Insert Table 3 about here
 =====

In the simulation design, the number of repetitions $S = 1,000$ is determined by an empirical method introduced in (Morris et al., 2019). We performed a pilot study and found that the standard errors of all coefficients except the parameters related to the initial status and vertical distance¹⁰ were below 0.15. Therefore, at least 900 repetitions are

¹⁰In the negative exponential function, the vertical distance is the distance between the initial status and asymptotic level while in the Jeness-Bayley function, it is the distance between the initial status and intercept of the linear asymptote.

needed to keep the Monte Carlo standard error of the bias¹¹ less than 0.005. For this reason, we determined to perform the simulation study with 1,000 replications for more conservative consideration.

3.1 Design of Simulation Study

We provide all the conditions that we considered for each model in the simulation design in Table 4. An important factor in models used to investigate longitudinal processes is the number of repeated measures. One hypothesis is that the model performs better as repeated records increase. We were interested in examining this hypothesis through the simulation study. Therefore, we selected two levels of repeated measures for all four models: six and ten. One goal was to assess whether the longitudinal records are equally-placed or not affect the model performance, assuming that we had the same study duration with ten repeated measurements. In addition, we wanted to see how these four models perform under the more challenging condition with shorter study duration and six repeated records. Moreover, we allowed for a ‘medium’ time window $(-0.25, +0.25)$ around each wave, following (Coulombe et al., 2015). In addition to the time structures, we also considered some same conditions across the four models. For example, we fixed the distribution of the initial status $(\eta_{0i} \sim N(50, 5^2))$ since it only affects the position of a trajectory. In addition, we set the growth factors in each model to be positively correlated to a moderate level $(\rho = 0.3)$ and considered two levels of sample size $(n = 200 \text{ or } 500)$ and two levels of residual variance $(\theta_\epsilon = 1 \text{ or } 2)$ for all four models.

=====
 Insert Table 4 about here
 =====

For the nonparametric LCSM (i.e., LBGm), we examined how the trajectory shape, quantified by the shape factor and relative rate-of-change, affects the model. As shown in Table 4, we fixed the distribution of shape factor and examined the trajectory with a decreasing or increasing rate-of-change in the simulation study. On the other hand, for the exponential LCSM and Jenss-Bayley LCSM, we only considered the nonlinear trajectory with a declining rate-of-change (i.e., the trajectory with an asymptotic level) because identifying the asymptote is one goal of using these parametric LCSMs. We fixed the vertical distance for the negative exponential LCSM to have a constant asymptote level but considered two levels of logarithmic ratio of the growth rate $(b = 0.4 \text{ or } 0.8)$. We fixed the vertical distance and the ratio of the growth acceleration for the Jenss-Bayley LCSM but examined how a different rate-of-change in the later developmental stage, quantified by the slope of the linear asymptote, affects model performance. Specifically, we considered two distributions of the slope of the linear asymptote, $N(2.5, 1.0^2)$ and $N(1.0, 0.4^2)$, for a large and small rate-of-change in the later stage. The change of the quadratic function is not monotonic, so we adjusted the linear and quadratic slopes to have a monotonic change of the study with six and ten repeated measurements.

3.2 Data Generation and Simulation Step

For each condition of each model listed in Table 4, we carried out the simulation study according to the following steps:

1. Generate growth factors for the LBGm and each parametric LGCM using the R package *MASS* Venables and Ripley (2002),
2. Generate the time structure with J waves t_j as specified in Table 4 and allow for disturbances around each wave $t_{ij} \sim U(t_j - \Delta, t_j + \Delta)$ $(\Delta = 0.25)$ to have individual measurement occasions,
3. Calculate factor loadings of each individual for the LBGm and each parametric LGCM, which are functions of the individual measurement occasions and the additional growth coefficient(s) (if applicable),
4. Calculate the values of the repeated measurements based on the growth factors, factor loadings, and residual variance,
5. Implement each LCSM and the corresponding LGCM (if applicable), estimate the parameters, and construct the corresponding 95% Wald confidence intervals,
6. Repeat the above steps until achieving 1,000 convergent solutions.

¹¹The most important performance metric in a simulation study is the bias, and equation for the Monte Carlo standard error is Monte Carlo $SE(\text{Bias}) = \sqrt{Var(\hat{\theta})/S}$ Morris et al. (2019).

4 Results

4.1 Model Convergence

We first evaluated the convergence¹² rate of each proposed model and the corresponding LGCM (if applicable). The proposed models and their available LGCM counterparts converged well as they reported a 100% convergence rate for all conditions listed in Table 4.

4.2 Performance Metrics

In this section, we examine the performance metrics of each parameter under all conditions for each LCSM, including relative bias, empirical SE, relative RMSE, and empirical coverage of the nominal 95% confidence interval. For each parameter of each model, we calculated each performance measure across 1,000 replications under each condition and summarized the values of each performance metric across all conditions into the corresponding median and range. In general, the models with the novel specification are capable of providing unbiased and accurate point estimates with target coverage probabilities. We provide these summaries in Tables 5-8.

=====
 Insert Table 5 about here
 =====

=====
 Insert Table 6 about here
 =====

=====
 Insert Table 7 about here
 =====

=====
 Insert Table 8 about here
 =====

Table 5 provides the summary of the nonparametric LCSM with the proposed specification. The LBGCM was able to generate unbiased point estimates and small empirical SEs. The magnitude of the relative biases of all parameters in the model was less than 0.02. In addition, except for the mean and variance of the intercept, the magnitude of the parameters' empirical SEs was less than 0.19 (the empirical SE of the intercept mean and variance were below 0.38 and 2.67, respectively). In addition, the estimates from the LBGCM were accurate: the magnitude of the relative RMSE of all parameters was lower than 0.29. In addition, the CPs of all parameters under all conditions that we considered in the simulation were around 0.95, indicating that the 95% confidence interval generated by the LBGCM covered the population value at the target level under each condition.

Table 6 provides the summary for the quadratic LCSM with the proposed specification. The performance of the quadratic LCSM was also satisfactory. Specifically, the magnitude of the relative biases and the relative RMSE of all parameters was less than 0.02 and 0.52, respectively. Moreover, except for the parameters related to the intercept, the magnitude of the empirical SE was below 0.25. Additionally, the CPs of all parameters under all conditions were sufficiently close to 0.95.

Table 7 lists the summary of the performance metrics of the negative exponential LCSM with the proposed specification. In general, the model performed satisfactorily. In particular, the magnitude of the relative biases of most parameters was below 0.01, although the relative bias of the mean and variance of the vertical distance was slightly larger, reaching 0.03 and 0.06, respectively. In addition, we noticed that the CP of the mean value of the vertical distance was not satisfied. Through further investigation, we found that the exponential LCSM worked better under the conditions with the small ratio of the growth rate (i.e., $b = 0.4$) and the long study duration with more early records (i.e., ten repeated measurements with unequally-spaced waves).

We provide the summary of the performance metrics for the Jenss-Bayley LCSM with the proposed specification in Table 8. The performance of this model was generally satisfactory. It can be seen from the table that the estimates of

¹²Convergence in the current project is defined as achieving the *OpenMx* status code 0 (which suggests that the optimization is successful) until up to 10 trials with different sets of starting values.

the parameters related to the asymptotic slope and vertical distance were not ideal, but they were still acceptable. With further examination, we noticed that the Jeness-Bayley LCSM performed better under the conditions with more repeated measurements, the time structure of unequally-spaced study waves, and the larger sample size.

4.3 Model Comparison

This section compares the model performance between each parametric LCSM and the corresponding LGCM based on the four measures and information criteria, including Akaike’s Information Criteria (AIC) and Bayesian Information Criteria (BIC). We provide the summary of the performance metrics of quadratic, exponential, and Jeness-Bayley LGCM in Tables 6, 7, and 8, respectively. Under each condition, we noticed that the point estimates of the quadratic LCSM and LGCM of each replication stayed consistent up to the fourth decimal place. Therefore, except for one cell, the performance metric summary tables of the two models were the same. Additionally, the estimated likelihood values of the two models were the same in all replications under all conditions up to four decimals, so were the AIC and BIC. This is what we expect: as shown in Equation 10 and Figure 2b, the rate-of-change of the quadratic function has a linear relationship with the time t , so the instantaneous slope halfway through a time interval is identical to the ARC in that period. To this end, the estimates of the quadratic LCSM are the same as those from the corresponding LGCM.

For the negative exponential function and Jeness-Bayley function, the LGCM outperformed the corresponding LCSM, especially in terms of parameter estimation related to the vertical distance (and the slope of linear asymptote of the Jeness-Bayley function). Specifically, although these point estimates from the LGCMs and LCSMs can be considered unbiased (i.e., relative biases are less than 10%), the bias from the LGCMs was still relatively smaller. As shown in Tables 7 and 8, the negative exponential LCSM and Jeness-Bayley LCSM tended to overestimate¹³ the vertical distance and slightly underestimate the additional coefficient (i.e., b or c). In addition, the Jeness-Bayley LCSM could underestimate the slope of the linear asymptote. This is not surprising. The negative exponential and Jeness-Bayley functions are growth curves with decreasing deceleration (i.e., negative acceleration). Therefore, the instantaneous slope halfway through a period is numerically smaller than the ARC in the time interval. For this reason, both models are likely to overestimate d_{ij_mid} to satisfy the specified functions. For the negative exponential LCSM, this results in an overestimated vertical distance¹⁴.

As shown in Equation 12, d_{ij_mid} of the Jeness-Bayley function consists of the linear asymptote slope and negative exponential term, and the estimation of the two terms is supposed to be complementary. So for the Jeness-Bayley function, an overestimated vertical distance led to an underestimated linear slope. In addition, since these point estimates from the LGCM were less biased, the CPs generated by the LGCM covered the population values better than the corresponding CPs from the LCSM. In addition, among all 24 conditions of the negative exponential (Jeness-Bayley) function, there were 13 (8) conditions where the difference in the BIC across all replications is less than 6¹⁵. For the remaining conditions, at least 63.0% (87.9%) replications reported a BIC difference that is less than 6.

To summarize, according to our simulation study, the estimates of all four models with the novel specification were unbiased and accurate, with the target 95% coverage probability in general. Some factors, such as the number of repeated measurements (the length of study duration) and the occasions of these measurements, might affect model performance. Specifically, more measurements, especially more measurements in an earlier stage, could improve the performance of these models. In the simulation study, we found that the negative exponential LGCM and Jeness-Bayley LGCM outperformed the corresponding LCSM, which is within our expectation since we fit the LGCM and LCSM to the corresponding LGCM-implied data structure. Even so, the overall performance of the LCSMs with the novel specification was still satisfactory.

5 Application

We now use empirical data to demonstrate how to apply the LCSMs with the novel specification and the corresponding LGCMs (if applicable) to answer research questions. This part of the application has two goals. The first goal is to provide a set of feasible recommendations on how to employ the proposed LCSMs and use the free and derived parameters to answer specific research questions. The second goal is to show how different frameworks with the same trajectory function affect the estimation in this real-world practice; for this reason, we built up the three LGCMs as a

¹³By ‘overestimate’, we mean that the point estimate is farther from zero than the population value. Similarly, by ‘underestimate’, we mean that the point estimate is closer to zero than the true value.

¹⁴As shown in Equation 11, d_{ij_mid} of the negative exponential growth curve is determined by the vertical distance and the coefficient b . Slightly underestimating the coefficient b (such as the relative bias below 0.01 in our LCSM case) does not affect the estimation of d_{ij_mid} numerically. Therefore, the overestimation of d_{ij_mid} leads to an overestimated vertical distance.

¹⁵(Raftery, 1995) has shown that a difference in BIC below 6 does not suggest strong evidence regarding the model preference.

sensitivity analysis. In this application, we randomly selected 400 students from The Early Childhood Longitudinal Study, Kindergarten Class of 2010-2011 (ECLS-K: 2011) with non-missing records of repeated reading assessments and age at each study wave¹⁶.

ECLS-K: 2011 is a nationwide longitudinal study starting from the 2010-2011 school year and collecting records from US children enrolled in approximately 900 kindergarten programs. In ECLS-K: 2011, the reading ability of students was evaluated in nine waves: each semester in kindergarten, first, and second grade, followed by once a school year (only spring semester) in third, fourth, and fifth grade. In the fall semester of 2011 and 2012, only about 30% of students were assessed Lê et al. (2011). In this analysis, we used the child’s age (in years) for each wave so that each student had different measurement times. Table 9 shows the mean and standard deviation of the observed item response theory (IRT) scores and the amounts of change-from-baseline of reading ability at each study wave.

5.1 Main Analysis

We fit the nonparametric and three parametric LCSMs with the novel specification to analyze the development of the students’ reading ability. All four models converged within half of a minute. We provide the estimated likelihood, AIC, BIC, variance of residual, and the number of parameters of each LCSM in Table 10. The table shows that the nonparametric LCSM (i.e., LBGm) outperformed three parametric LCSMs from the statistical perspective since it has the largest estimated likelihood and the smallest values of information criteria, including the AIC and BIC. This is not surprising: the model without a pre-specified functional form tends to capture the data structure better, which, in turn, implies a larger likelihood.

Table 11 presents the estimates of parameters of the LBGm. As introduced earlier, we scaled η_1 as the growth rate in the first time interval of the developmental process of reading ability. That is, the parameters related to the initial status and the growth rate in the first interval as well as the values of relative rate-of-change were directly estimated from the proposed model, while the mean and variance of the absolute rate-of-change during each time interval were derived using the function *mxAlgebra()* with *mxEval()* and *mxSE()*. Furthermore, the estimated variability of the initial status and rate-of-change was significant, suggesting the students had individual intercepts and slopes, and thus, individual growth trajectories. In addition, there was a gradual slowdown in the development of reading skills since the growth rate declined over time. Specifically, reading ability development slowed down post-Grade 3 in general. Therefore, it suggests that the parametric functions with an asymptotic level, such as the negative exponential or Jeness-Bayley growth curves, can be employed to identify each student’s capacity of reading ability.

The estimates of the parametric LCSMs are summarized in Tables 12-14. For each parametric functional form, the output of the LCSM includes the estimates of the growth coefficients that are also available in the corresponding LGCM. In addition, we can obtain the estimated mean and variance of the instantaneous slope midway in each time interval as shown in Tables 12-14. The mean values of rate-of-change were not constant but declined with age. It is also noticed that the rate-of-change of the quadratic LCSM decreased linearly while the deceleration of the negative exponential and Jeness-Bayley LCSM was decreasing. In addition, all three parametric LCSMs suggested significant individual differences in the rate-of-change in reading ability development. For the quadratic and Jeness-Bayley LCSM, the variability of the rate-of-change first decreased and then increased, while for the negative exponential LCSM, the variability declined monotonically.

Another important output of the LCSM is the amount of change-from-baseline at each post-baseline time point, which is a commonly used metric to evaluate a change in an observational study or a treatment effect in an intervention study. In Figure 4, we plot the model-implied change-from-baseline on the smooth line of the corresponding observed values of the reading IRT scores for each proposed LCSM. It can be seen from the figure that the estimated values of change-from-baseline from all three parametric LCSMs can capture the observed values well.

5.2 Sensitivity Analysis

We built up the corresponding LGCM for each LCSM as a sensitivity analysis. The estimated likelihood, AIC, BIC, and residual variance of each LGCM are also provided in Table 10. From the table, we noticed that the values of AIC and BIC of the LGCM were smaller than the corresponding values of LCSM. In addition, we derived the values of change-from-baseline for the three LGCMs and provided the LGCM-based change-from-baseline in Figure 4. We noticed from the figure that the LGCMs tended to overestimate the amount of change-from-baseline. One possible reason for the poor performance of the LGCM in estimating the amount of change-from-baseline in this application is that all three models underestimated the intercept means (the estimated mean of the initial status was 38.317, 32.295

¹⁶There are $n = 18174$ participants in ECLS-K: 2011. After removing rows with missing values (i.e., records with any of $NaN / -9 / -8 / -7 / -1$), we have $n = 3418$ students.

and 33.586 from the quadratic, negative exponential, and Jentsch-Bayley LGCM, respectively). In the Discussion section, we will further explain the implication of such differences in the information criteria and the estimation of the amount of change-from-baseline.

6 Discussion

This article extends the existing LCSM framework to allow for unstructured measurement occasions. Specifically, we view the growth over time as the AUC of the $r - t$ graph and, for the parametric LCSM, we propose to approximate the latent change score (i.e., the AUC) within a time interval as the product of the instantaneous slope midway through the interval and the length of the interval. We examined four LCSMs with the proposed specification through extensive simulation studies. Based on our results, with the novel specification, the nonparametric LCSM is capable of providing unbiased and accurate point estimates with target coverage probabilities. For each parametric LCSM, we generated LGCM-implied data structures and constructed the corresponding LGCM and LCSM. Based on our examination, the parametric LCSM with the novel specification is an ideal alternative to the corresponding LGCM in general. Additionally, we apply the proposed models to analyze the developmental process of reading ability using a subsample of $n = 400$ from ECLS-K: 2011.

6.1 Practical Considerations

This section provides a set of recommendations for empirical researchers based on the simulation study and real-world data analysis. First, it is not our aim to demonstrate that the LCSM framework is universally preferred, although the proposed novel specification of the LCSM has multiple good features such as allowing for unequally-spaced study waves and individual measurement occasions around each wave. If the research interest only focuses on analyzing the observed longitudinal outcomes, we recommend using the LGCM because the simulation study has shown that the parametric LGCM slightly outperforms the corresponding LCSM in some challenging conditions. In addition, the model specification of the LGCM is more straightforward, and therefore, the interpretation of the output is more explicit. However, if the research interest is to examine change, such as the rate-of-change or the amount of the change-from-baseline, the LCSM framework is a great candidate. As demonstrated in the Application section, the LCSM can also estimate the means and variances of the instantaneous slope over time, which allows us to examine between-individual differences in within-individual changes in nonlinear trajectories.

Additionally, as shown in the Application section, a parametric LGCM fit the data better (i.e., the greater estimated likelihood) but generated poorer estimates of the change-from-baseline than the corresponding LCSM. One possible explanation is that no functional forms we considered in this analysis can perfectly capture the underlying change pattern of these trajectories, which is typical in any real-world analysis. Specifically, we utilize a pre-specified functional form to capture the observed longitudinal records when specifying a parametric LGCM. As a result, the estimates of growth coefficients from the LGCM fit the majority of observed values well. For example, the LGCM underestimated the initial status in our case, but the estimated coefficients fit the post-baseline observed values well; therefore, it overestimated the amount of the change-from-baseline. However, when specifying the corresponding LCSM, we employ the first derivative of the function, which is unrelated to the initial status, to constrain the pattern of rate-of-change. To this end, the estimates of growth coefficients from the LCSM fit the observed initial status and the first derivative values well.

Moreover, the selection of the time unit affects the estimates of the nonlinear trajectories, especially for the growth coefficient b in the negative exponential function and c in the Jentsch-Bayley growth curve, since b and c measures the ratio of the growth rate and the ratio of the growth acceleration at two consecutive time points, respectively, and therefore, varies with the time unit. In practice, we recommend using a relatively large time unit (for example, age-in-year instead of age-in-month in the Application section) to observe a reasonable effect size and ensure the interpretation of these coefficients is meaningful to empirical studies.

6.2 Methodological Considerations and Future Directions

This article introduces the novel specification for the LCSM to allow for individual measurement occasions and demonstrates how to apply this proposed specification to fit the LCSM with nonparametric and parametric functional forms. When fitting the LCSM with the negative exponential and Jentsch-Bayley functions, we assume that the growth coefficients b and c are roughly the same across individuals to build a parsimonious model. However, these growth coefficients could also be individually different, as stated earlier. Accordingly, one possible future extension is to relax the assumption of the fixed growth rate ratio or growth acceleration ratio and examine their random effects to assess individual-level ratio in the LCSM framework as an application warrants. In addition, the novel specification of the

latent change score can also be extended to other commonly used LCSMs, such as the proportional change model and the dual change model.

Moreover, one benefit of the LCSM is that it can estimate the amount of the change-from-baseline at each post-baseline time point. In addition to using this metric to evaluate the amount of change in one group, researchers may also be interested in comparing the change of multiple manifested or latent groups. Therefore, it is worth extending the LCSM with the novel specification to the multiple-groups framework or finite mixture modeling framework to examine these between-groups differences in the amount of change over time.

In addition, as shown in the Application section, the nonparametric LCSM tends to estimate the change-related parameters and capture the data structure well but fails to provide coefficients related to developmental theory (for example, an asymptotic level to suggest capacity). On the contrary, the parametric LCSMs can estimate the coefficients that allow for making hypotheses, yet they may not capture the data structure well. One possible extension is to develop semi-parametric LCSMs, such as a LCSM with a linear-quadratic piecewise function or linear-negative exponential piecewise function. Last, although we demonstrate the LCSMs with the novel specification with complete longitudinal records, it is possible to extend the current work to address a longitudinal data set with dropout under the assumption of missing at random thanks to the FIML technique.

6.3 Concluding Remarks

This article views the growth curve as the AUC under the $r - t$ graph and proposes a novel specification for the LCSM with one nonparametric and multiple parametric nonlinear functions. The novel specification allows for unequally-spaced study waves and individual measurement occasions around each wave. Other than the information provided by the LGCM, the LCSM is also capable of estimating the means and variances of the instantaneous slope midway in each time interval and the amount of change-from-baseline at each post-baseline time point. The simulation study and application demonstrate the specification's valuable capabilities of estimating all parameters related to change. Furthermore, as discussed above, the proposed specification can be generalized in practice and further examined in methodology.

References

- Bauer, D. J. (2003). Estimating multilevel linear models as structural equation models. *Journal of Educational and Behavioral Statistics*, 28(2):135–167.
- Biesanz, J. C., Deeb-Sossa, N., Papadakis, A. A., Bollen, K. A., and Curran, P. J. (2004). The role of coding time in estimating and interpreting growth curve models. *Psychological methods*, 9(1):30–52.
- Blozis, S. A. and Cho, Y. (2008). Coding and centering of time in latent curve models in the presence of interindividual time heterogeneity. *Structural Equation Modeling: A Multidisciplinary Journal*, 15(3):413–433.
- Boker, S. M., Neale, M. C., Maes, H. H., Wilde, M. J., Spiegel, M., Brick, T. R., Estabrook, R., Bates, T. C., Mehta, P., von Oertzen, T., Gore, R. J., Hunter, M. D., Hackett, D. C., Karch, J., Brandmaier, A. M., Pritikin, J. N., Zahery, M., and Kirkpatrick, R. M. (2020). *OpenMx 2.17.2 User Guide*.
- Bollen, K. A. and Curran, P. J. (2005). *Latent Curve Models*. John Wiley & Sons, Inc.
- Bollen, K. A. and Curran, P. J. (2006). *Latent Curve Models*. John Wiley & Sons, Inc.
- Browne, M. W. and du Toit, S. H. C. (1991). Models for learning data. In Collins, L. M. and Horn, J. L., editors, *Best methods for the analysis of change: Recent advances, unanswered questions, future directions*, chapter 4, pages 47–68. American Psychological Association., Washington, DC, US.
- Bryk, A. S. and Raudenbush, S. W. (1987). Application of hierarchical linear models to assessing change. *Psychological Bulletin*, 101(1):147–158.
- Coulombe, P., Selig, J. P., and Delaney, H. D. (2015). Ignoring individual differences in times of assessment in growth curve modeling. *International Journal of Behavioral Development*, 40(1):76–86.
- Curran, P. J. (2003). Have multilevel models been structural equation models all along? *Multivariate Behavioral Research*, 38(4):529–569.
- Driver, C. C., Oud, J. H. L., and Voelkle, M. C. (2017). Continuous time structural equation modeling with r package ctsem. *Journal of Statistical Software*, 77(5):1–35.
- Driver, C. C. and Voelkle, M. C. (2018). Hierarchical bayesian continuous time dynamic modeling. *Psychological Methods*, 23(4):774–799.

- Duncan, S. C., Duncan, T. E., and Strycker, L. A. (2000). Risk and protective factors influencing adolescent problem behavior: A multivariate latent growth curve analysis. *Annals of Behavioral Medicine*, 22(2):103.
- Duncan, T. E., Duncan, S. C., and Strycker, L. A. (2013). *An Introduction to Latent Variable Growth Curve Modeling: Concepts, Issues, and Application (2nd)*. Routledge.
- Estabrook, R. and Neale, M. (2013). A comparison of factor score estimation methods in the presence of missing data: Reliability and an application to nicotine dependence. *Multivariate behavioral research*, 48(1):1–27.
- Finkel, D., Reynolds, C., Mcardle, J., Gatz, M., and L Pedersen, N. (2003). Latent growth curve analyses of accelerating decline in cognitive abilities in late adulthood. *Developmental psychology*, 39:535–550.
- Grimm, K. J., Castro-Schilo, L., and Davoudzadeh, P. (2013a). Modeling intraindividual change in nonlinear growth models with latent change scores. *GeroPsych: The Journal of Gerontopsychology and Geriatric Psychiatry*, 26(3):153–162.
- Grimm, K. J. and Jacobucci, R. (2018). Individually varying time metrics in latent change score models. In Ferrer, E., Boker, S., and Grimm, K. J., editors, *Longitudinal Multivariate Psychology*, chapter 3, pages 61–79. Guilford Press.
- Grimm, K. J., Ram, N., and Estabrook, R. (2016). *Growth Modeling: Structural Equation and Multilevel Modeling Approaches*. Guilford Press.
- Grimm, K. J., Ram, N., and Hamagami, F. (2011). Nonlinear growth curves in developmental research. *Child development*, 82(5):1357–1371.
- Grimm, K. J., Zhang, Z., Hamagami, F., and Mazzocco, M. (2013b). Modeling nonlinear change via latent change and latent acceleration frameworks: Examining velocity and acceleration of growth trajectories. *Multivariate Behavioral Research*, 48(1):117–143.
- Grimm, K. J., Zhang, Z., Hamagami, F., and Mazzocco, M. (2013c). Modeling nonlinear change via latent change and latent acceleration frameworks: Examining velocity and acceleration of growth trajectories. *Multivariate Behavioral Research*, 48(1):117–143.
- Harville, D. A. (1977). Maximum likelihood approaches to variance component estimation and to related problems. *Journal of the American Statistical Association*, 72(358):320–338.
- Hedeker, D. and Gibbons, R. D. (2006). *Longitudinal Data Analysis*. Wiley Series in Probability and Statistics. Wiley.
- Hunter, M. D. (2018). State space modeling in an open source, modular, structural equation modeling environment. *Structural Equation Modeling*, 25(2):307–324.
- Kelley, K. (2009). The average rate of change for continuous time models. *Behavior Research Methods*, 41:268–278.
- Kelley, K. and Maxwell, S. E. (2008). Delineating the average rate of change in longitudinal models. *Journal of Educational and Behavioral Statistics*, 33(3):307–332.
- Laird, N. M. and Ware, J. H. (1982). Random-effects models for longitudinal data. *Biometrics*, 38:963–974.
- Lê, T., Norman, G., Tourangeau, K., Brick, J. M., and Mulligan, G. (2011). Early childhood longitudinal study: Kindergarten class of 2010–2011 - sample design issues. In *JSM Proceedings 2011*, pages 1629–1639, Alexandria, VA. American Statistical Association.
- Lehmann, E. L. and Casella, G. (1998). *Theory of Point Estimation, 2nd edition*. Springer-Verlag New York, Inc.
- Lindstrom, M. J. and Bates, D. M. (1990). Nonlinear mixed effects models for repeated measures data. *Biometrics*, 46(3):673–687.
- Liu, J., Perera, R. A., Kang, L., Kirkpatrick, R. M., and Sabo, R. T. (2021). Obtaining interpretable parameters from reparameterizing longitudinal models: transformation matrices between growth factors in two parameter spaces. *Journal of Educational and Behavioral Statistics*.
- McArdle, J. J. (1986). Latent variable growth within behavior genetic models. *Behavior Genetics*, 16(1):163–200.
- McArdle, J. J. (2001). A latent difference score approach to longitudinal dynamic structural analysis. In Cudeck, R., du Toit, S. H. C., and Sorbom, D., editors, *Structural equation modeling: Present and future*, pages 342–380. Lincolnwood, IL: Scientific Software International.
- McArdle, J. J. (2009). Latent variable modeling of differences and changes with longitudinal data. *Annual review of psychology*, 60:577–605.
- McArdle, J. J. and Hamagami, F. (2001). Latent difference score structural models for linear dynamic analyses with incomplete longitudinal data. In Collins, L. M. and Sayer, A. G., editors, *Decade of behavior. New methods for the analysis of change*, page 139–175. American Psychological Association.

- Mehta, P. D. and Neale, M. C. (2005). People are variables too: Multilevel structural equations modeling. *Psychological Methods*, 10(3):259–284.
- Mehta, P. D. and West, S. G. (2000). Putting the individual back into individual growth curves. *Psychological Methods*, 5(1):23–43.
- Meredith, W. and Tisak, J. (1990). Latent curve analysis. *Psychometrika*, 55(1):107–122.
- Morris, T. P., White, I. R., and Crowther, M. J. (2019). Using simulation studies to evaluate statistical methods. *Statistics in Medicine*, 38(11):2074–2102.
- Neale, M. C., Hunter, M. D., Pritikin, J. N., Zahery, M., Brick, T. R., Kirkpatrick, R. M., Estabrook, R., Bates, T. C., Maes, H. H., and Boker, S. M. (2016). OpenMx 2.0: Extended structural equation and statistical modeling. *Psychometrika*, 81(2):535–549.
- Pinheiro, J. C. (1994). *Topics in Mixed Effects Models*. University of Wisconsin-Madison.
- Preacher, K. J. and Hancock, G. R. (2012). On interpretable reparameterizations of linear and nonlinear latent growth curve models. In Harring, J. R. and Hancock, G. R., editors, *CILVR series on latent variable methodology. Advances in longitudinal methods in the social and behavioral sciences*, chapter 2, pages 25–58. IAP Information Age Publishing, Charlotte, NC, US.
- Preacher, K. J. and Hancock, G. R. (2015). Meaningful aspects of change as novel random coefficients: A general method for reparameterizing longitudinal models. *Psychological Methods*, 20(1):84–101.
- Pritikin, J. N., Hunter, M. D., and Boker, S. M. (2015). Modular open-source software for Item Factor Analysis. *Educational and Psychological Measurement*, 75(3):458–474.
- Raftery, A. (1995). Bayesian model selection in social research. *Sociological Methodology*, 25:111–163.
- Ram, N. and Grimm, K. J. (2007). Using simple and complex growth models to articulate developmental change: Matching theory to method. *International Journal of Behavioral Development*, 31(4):303–316.
- Rao, R. C. (1958). Some statistical methods for comparison of growth curves. *Biometrics*, 14(1):1–17.
- Sterba, S. K. (2014). Fitting nonlinear latent growth curve models with individually varying time points. *Structural Equation Modeling: A Multidisciplinary Journal*, 21(4):630–647.
- Tucker, L. R. (1958). Determination of parameters of a functional relation by factor analysis. *Psychometrika*, 23(1):19–23.
- Venables, W. N. and Ripley, B. D. (2002). *Modern Applied Statistics with S*. Springer, New York, fourth edition.
- Vonesh, E. F. and Carter, R. L. (1992). Mixed-effects nonlinear regression for unbalanced repeated measures. *Biometrics*, 48(1):1–17.
- Zhang, Z., McArdle, J. J., and Nesselroade, J. R. (2012). Growth rate models: emphasizing growth rate analysis through growth curve modeling. *Journal of Applied Statistics*, 39(6):1241–1262.

Appendix A Derivation of the Mean and Variance of the Rate-of-Change

This section provides the detailed derivation for the mean and variance of the rate of change (dy_{ij} in the LBGGM or dy_{ij_mid} in each parametric nonlinear LCSM). For the LBGGM, we have $dy_{ij} = \eta_{1i} \times \gamma_{j-1}$ ($j = 2, \dots, J$) from Equation 5. Suppose $f : \mathcal{R} \rightarrow \mathcal{R}$ is a function¹⁷, which takes a point $\eta_i \in \mathcal{R}$ as input and produces $f(\eta_i) \in \mathcal{R}$ as output. By the Delta method, the mean and variance of the rate-of-change of the LBGGM can be expressed as $\mu_{dy_{ij}} = \mu_{\eta_1} \times \gamma_j$ and $\phi_{dy_{ij}} = \psi_{11} \times \gamma_j^2$, respectively. Similarly, the mean and variance of the rate-of-change of each parametric LCSM can be expressed as¹⁸

- Quadratic Function:

$$\begin{aligned}\mu_{dy_{ij_mid}} &= \mu_{\eta_1} + 2 \times \mu_{\eta_2} \times t_{ij_mid}, \\ \phi_{dy_{ij_mid}} &= \psi_{11} + 4 \times \psi_{22} \times t_{ij_mid}^2 + 4 \times \psi_{12} \times t_{ij_mid},\end{aligned}$$

¹⁷In this project, f is a linear function. Under this scenario, the mean and variance can be derived using the theorem for calculating the mean and variance of linear combinations. The results obtained by the theorem and the Delta Method are identical.

¹⁸In the framework of individual measurement occasions, we consider t_{ij_mid} as the average value of the middle of two consecutive measurement times across all individuals to simplify the calculation of the mean and variance of the rate-of-change for the parametric LCSMs.

- Negative Exponential Function:

$$\begin{aligned}\mu_{dy_{ij_mid}} &= b \times \mu_{\eta_1} \times \exp(-b \times t_{ij_mid}), \\ \phi_{dy_{ij_mid}} &= [b \times \exp(-b \times t_{ij_mid})]^2 \times \psi_{11},\end{aligned}$$

- Jeness-Bayley function:

$$\begin{aligned}\mu_{dy_{ij_mid}} &= \mu_{\eta_1} + c \times \mu_{\eta_2} \times \exp(c \times t_{ij_mid}), \\ \phi_{dy_{ij_mid}} &= \psi_{11} + [c \times \exp(c \times t_{ij_mid})]^2 \times \psi_{22} + 2 \times c \times \psi_{12} \times \exp(c \times t_{ij_mid}).\end{aligned}$$

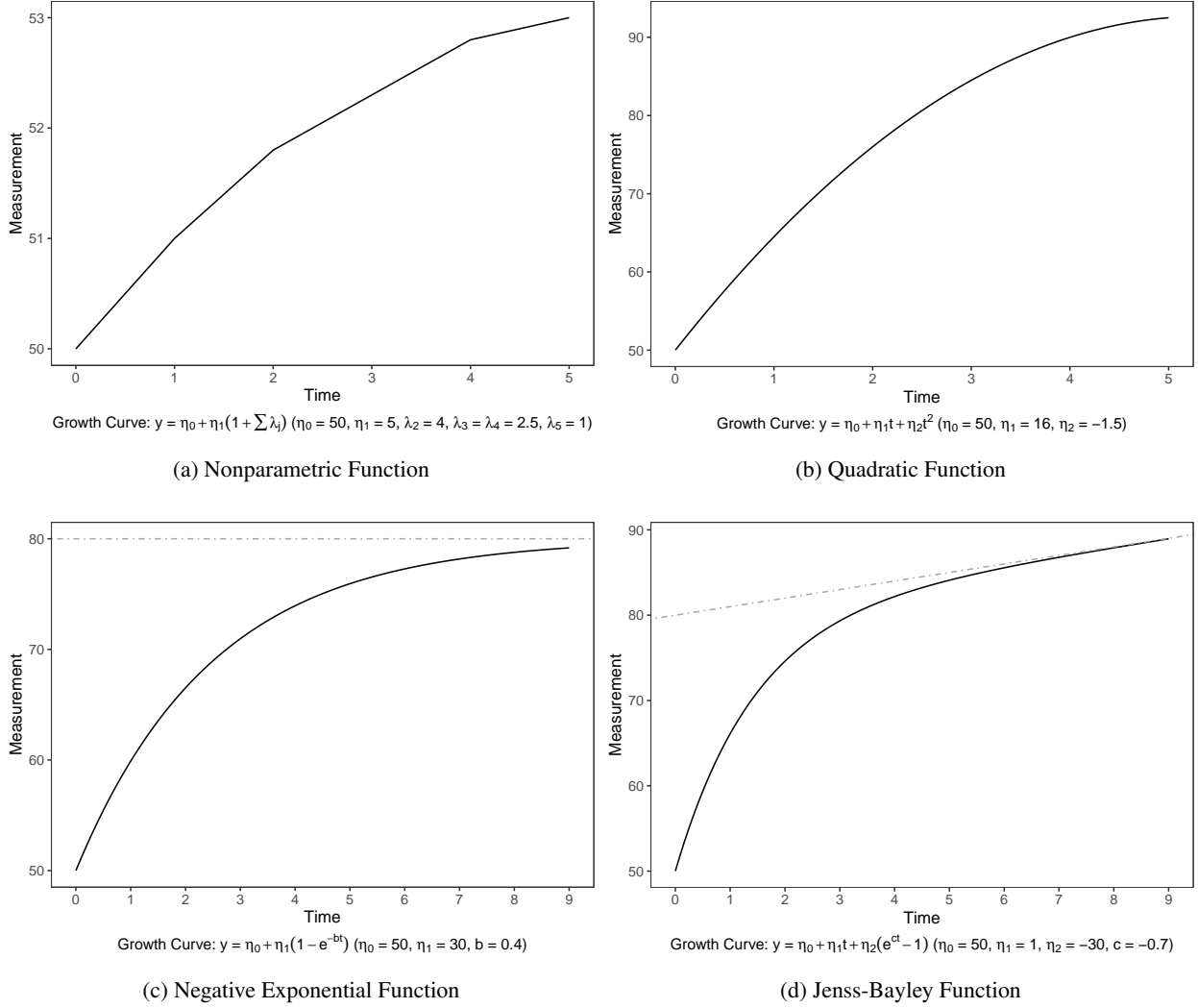


Figure 1: Growth versus Time Graph of Latent Growth Curve Models

Table 1: Summary of Latent Growth Curve Models with Commonly Used nonlinear Functional Forms

Functional Forms	Time-dependent Growth Status
Nonparametric Function	$y_{ij} = \eta_{0i} + \eta_{1i}(1 + \sum_{j=2}^{J-1} \lambda_j) + \epsilon_{ij}$
Quadratic Function	$y_{ij} = \eta_{0i} + \eta_{1i} \times t_j + \eta_{2i} \times t_j^2 + \epsilon_{ij}$
Negative Exponential Function	$y_{ij} = \eta_{0i} + \eta_{1i} \times (1 - \exp(-b \times t_j)) + \epsilon_{ij}$
Jenss-Bayley function	$y_{ij} = \eta_{0i} + \eta_{1i} \times t_j + \eta_{2i} \times (\exp(c \times t_j) - 1) + \epsilon_j$

Table 2: Summary of Latent Change Score Models with Commonly Used nonlinear Functional Forms

Functional Forms	Time-dependent Growth Change
Nonparametric Function	$d_{ij} = a_j \times \eta_{1i}$
Quadratic Function	$d_{ij} = \eta_{1i} + 2 \times \eta_{2i} \times t_j$
Negative Exponential Function	$d_{ij} = b \times \eta_{1i} \times \exp(-b \times t_j)$
Jenss-Bayley function	$d_{ij} = \eta_{1i} + c \times \eta_{2i} \times \exp(c \times t_j)$

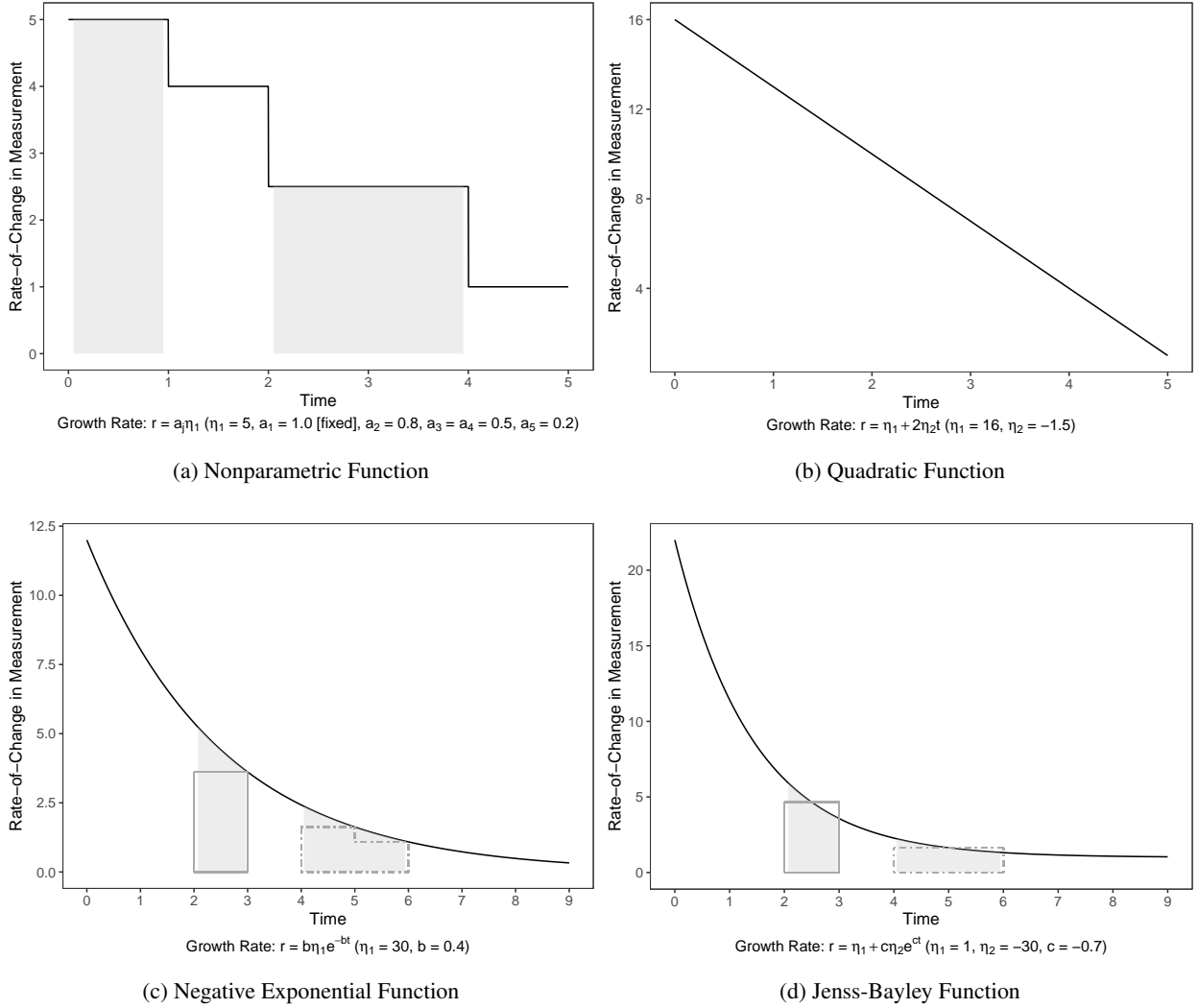


Figure 2: Rate-of-Change versus Time Graph of Latent Change Score Models

Table 3: Performance Measures for Evaluating an Estimate ($\hat{\theta}$) of Parameter (θ)

Criteria	Definition	Estimate
Relative Bias	$E_{\hat{\theta}}(\hat{\theta} - \theta)/\theta$	$\frac{\sum_{s=1}^S (\hat{\theta}_s^a - \theta)/\theta S^b}{S}$
Empirical SE	$\sqrt{Var(\hat{\theta})}$	$\sqrt{\frac{\sum_{s=1}^S (\hat{\theta}_s - \bar{\theta}^c)^2}{(S-1)}}$
Relative RMSE	$\sqrt{E_{\hat{\theta}}(\hat{\theta} - \theta)^2/\theta}$	$\sqrt{\frac{\sum_{s=1}^S (\hat{\theta}_s - \theta)^2/S/\theta}{S}}$
Coverage Probability	$Pr(\hat{\theta}_{lower} \leq \theta \leq \hat{\theta}_{upper})$	$\frac{\sum_{s=1}^S I(\hat{\theta}_{lower,s} \leq \theta \leq \hat{\theta}_{upper,s})^d}{S}$

^a $\hat{\theta}_s$: the estimate of θ from the s^{th} replication

^b S : the number of replications and set as 1,000 in our simulation study

^c $\bar{\theta}$: the mean of $\hat{\theta}_s$'s across replications

^d $I(\cdot)$: an indicator function

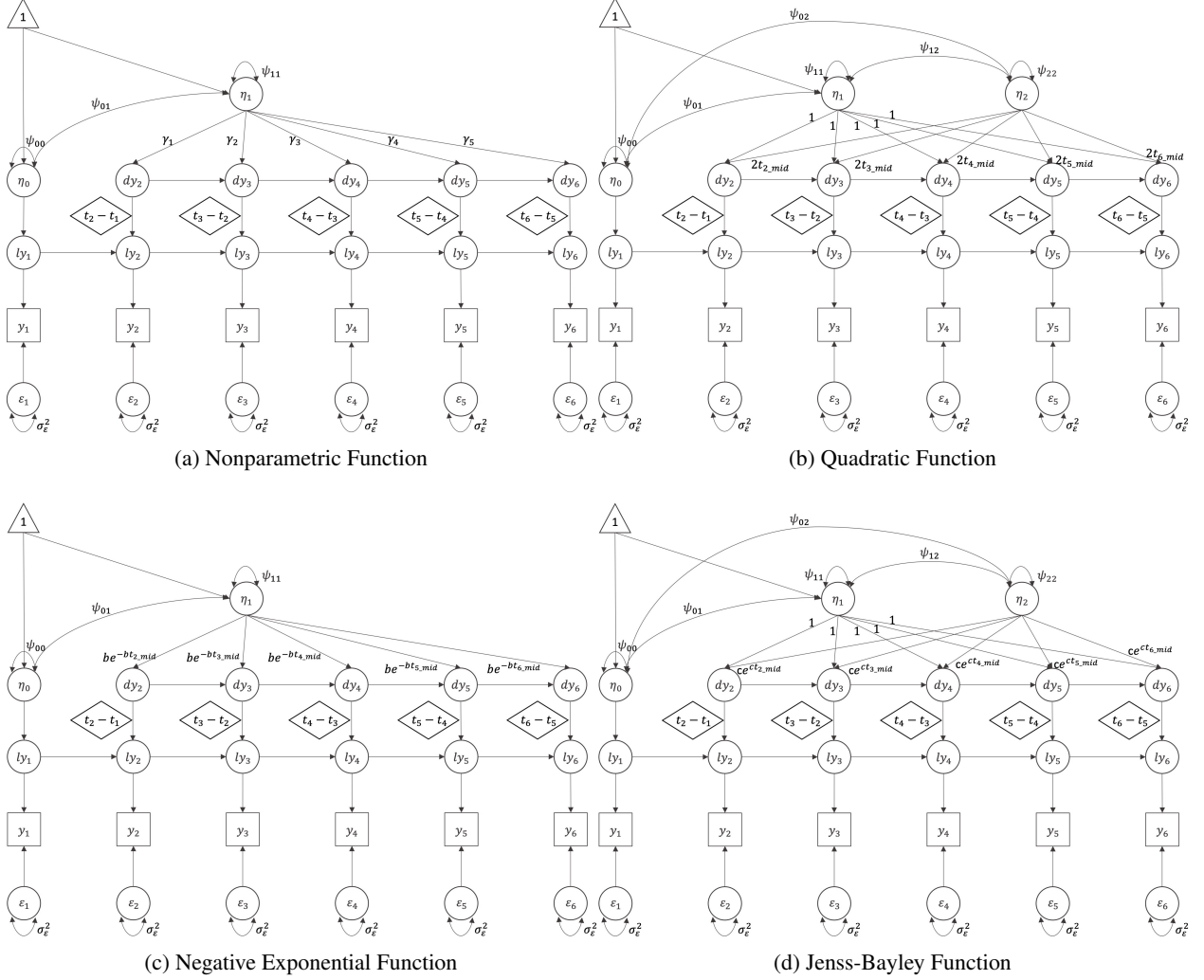


Figure 3: Path Diagram of Latent Change Score Models with the Novel Specification

Note: boxes=manifested variables, circles=latent variables, single arrow=regression paths; doubled arrow=(co)variances; triangle=constant; diamonds=definition variables.

In Figure 3a, we set $\gamma_1 = 1$ for model identification considerations.

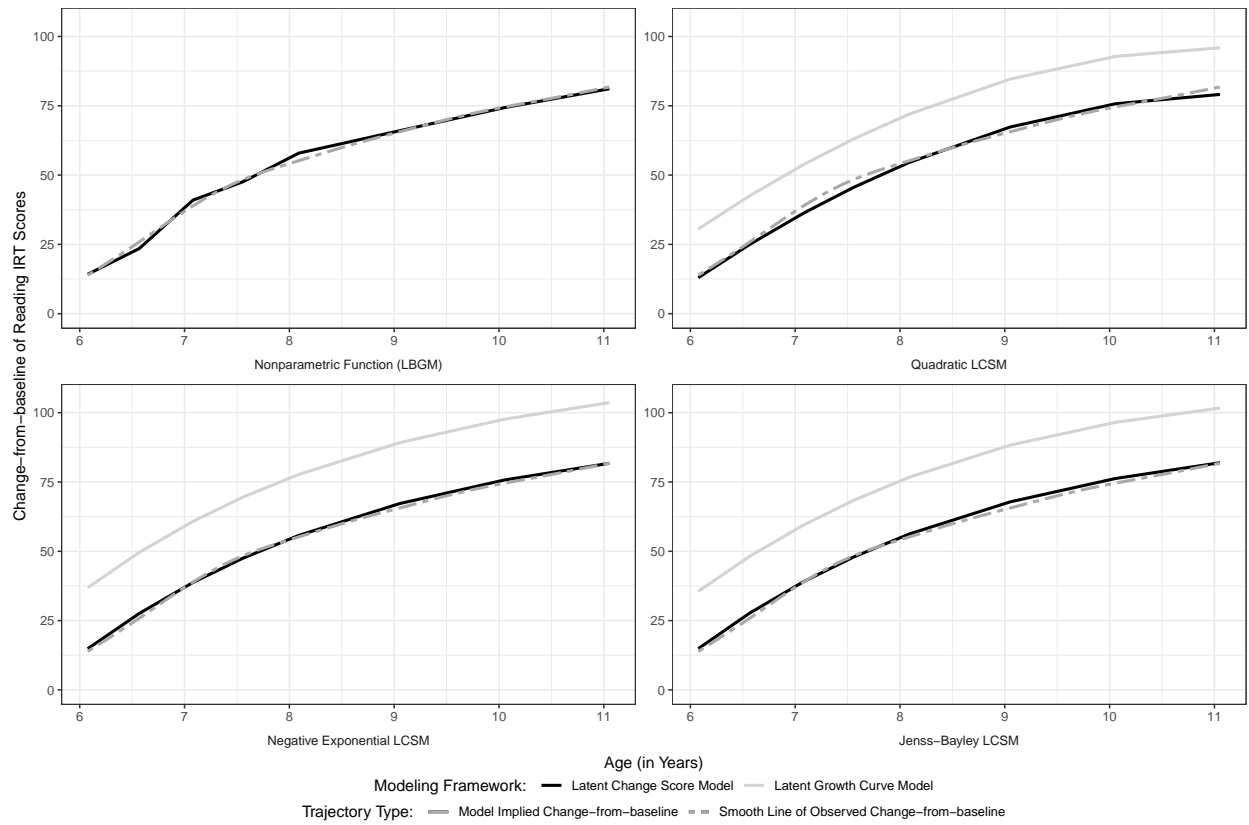


Figure 4: Model Implied Change-from-baseline and Smooth Line of Observed Change-from-baseline

Table 4: Simulation Design for Each Latent Change Score Model in the Framework of Individual Measurement Occasions

Common Conditions across Four Models	
Intercept	$\eta_{0i} \sim N(50, 5^2)$ (i.e., $\mu_{\eta_0} = 50, \psi_{00} = 25$)
Correlations of Growth Factors	$\rho = 0.3$
Time (t_j)	6 equally-spaced: $t_j = 0, 1.00, 2.00, 3.00, 4.00, 5.00$ 10 equally-spaced: $t_j = 0, 1.00, 2.00, 3.00, 4.00, 5.00, 6.00, 7.00, 8.00, 9.00$ 10 unequally-spaced: $t_j = 0, 0.75, 1.50, 2.25, 3.00, 3.75, 4.50, 6.00, 7.50, 9.00$
Individual t_{ij}	$t_{ij} \sim U(t_j - \Delta, t_j + \Delta)$ ($\Delta = 0.25$)
Sample Size	$n = 200, 500$
Residual Variance	$\theta_\epsilon = 1, 2$
Latent Change Score Model with Nonparametric Function	
Variables	Conditions
Shape Factor	$\eta_{1i} \sim N(3.0, 1.0^2)$ (i.e., $\mu_{\eta_1} = 3, \psi_{11} = 1$) 6 waves: $\gamma_1 = 1.0$ (fixed), $\gamma_{2/3/4/5} = 0.8/0.6/0.4/0.2$
Relative Rate-of-Change ^a	6 waves: $\gamma_1 = 1.0$ (fixed), $\gamma_{2/3/4/5} = 1.2/1.4/1.6/1.8$ 10 waves: $\gamma_1 = 1.0$ (fixed), $\gamma_{2/3/4/5/6/7/8/9} = 0.9/0.8/0.7/0.6/0.5/0.4/0.3/0.2$ 10 waves: $\gamma_1 = 1.0$ (fixed), $\gamma_{2/3/4/5/6/7/8/9} = 1.1/1.2/1.3/1.4/1.5/1.6/1.7/1.8$
Latent Change Score Model with Quadratic Function	
Variables	Conditions
Linear Slope	6 waves: $\eta_{1i} \sim N(16.0, 1.0^2)$ (i.e., $\mu_{\eta_1} = 16, \psi_{11} = 1$) 10 waves: $\eta_{1i} \sim N(20.0, 1.0^2)$ (i.e., $\mu_{\eta_1} = 20, \psi_{11} = 1$)
Quadratic Slope	6 waves: $\eta_{2i} \sim N(-1.5, 0.3^2)$ (i.e., $\mu_{\eta_2} = -1.5, \psi_{22} = 0.09$) 10 waves: $\eta_{2i} \sim N(-1.0, 0.3^2)$ (i.e., $\mu_{\eta_2} = -1.0, \psi_{22} = 0.09$)
Latent Change Score Model with Negative Exponential Function	
Vertical Distance ^b	$\eta_{1i} \sim N(30, 3.0^2)$ (i.e., $\mu_{\eta_1} = 30.0, \psi_{11} = 9.0$)
Log-ratio of Growth Rate	$b = 0.4, 0.8$
Latent Change Score Model with Jeness-Bayley Function	
Vertical Distance ^c	$\eta_{2i} \sim N(-30, 3.0^2)$ (i.e., $\mu_{\eta_2} = -30, \psi_{22} = 25$)
Slope of the Linear Asymptote	$\eta_{1i} \sim N(2.5, 1.0^2)$ (i.e., $\mu_{\eta_1} = 2.5, \psi_{11} = 1.00$)
Log-ratio of Growth Acceleration	$\eta_{1i} \sim N(1.0, 0.4^2)$ (i.e., $\mu_{\eta_1} = 1.0, \psi_{11} = 0.16$)
	$c = -0.7$ (i.e., $\exp(c) = 0.5$)

^a Relative rate-of-change is defined as the absolute rate-of-change over the shape factor.

^b Vertical distance in the negative exponential function is the distance between the intercept (i.e., the initial status) and the asymptotic level.

^c Vertical distance in the Jeness-Bayley function is the distance between the intercept (i.e., the initial status) and the intercept of the linear asymptote.

Table 5: Summary of Performance Metrics of Nonparametric Latent Change Score Model (Latent Basis Growth Model)

Para.	Relative Bias	Empirical SE ^a	Relative RMSE ^b	Coverage Probability
μ_{η_0}	0.0000 (-0.0005, 0.0003)	0.2963 (0.2186, 0.3774)	0.0060 (0.0044, 0.0075)	0.9500 (0.9400, 0.9620)
μ_{η_1}	-0.0002 (-0.0015, 0.0027)	0.1162 (0.0728, 0.1868)	0.0387 (0.0244, 0.0622)	0.9475 (0.9390, 0.9590)
ψ_{00}	-0.0030 (-0.0098, 0.0014)	2.0817 (1.5252, 2.6675)	0.0833 (0.0610, 0.1067)	0.9455 (0.9350, 0.9660)
ψ_{01}	-0.0049 (-0.0155, 0.0074)	0.3091 (0.2254, 0.4365)	0.2060 (0.1503, 0.2909)	0.9500 (0.9320, 0.9620)
$\psi_{1\downarrow}$	-0.0010 (-0.0085, 0.0056)	0.1092 (0.0748, 0.1597)	0.1092 (0.0745, 0.1595)	0.9460 (0.9230, 0.9540)
γ_2^c	0.0009 (-0.0034, 0.0063)	0.0524 (0.0300, 0.0985)	0.0558 (0.0312, 0.1033)	0.9490 (0.9290, 0.9630)
γ_3^c	0.0008 (-0.0038, 0.0053)	0.0464 (0.0245, 0.0854)	0.0480 (0.0237, 0.0921)	0.9490 (0.9380, 0.9660)
γ_4^c	0.0013 (-0.0026, 0.0051)	0.0458 (0.0224, 0.0922)	0.0506 (0.0234, 0.1157)	0.9480 (0.9280, 0.9610)
γ_5^c	0.0013 (-0.0023, 0.0057)	0.0458 (0.0200, 0.0954)	0.0505 (0.0229, 0.2282)	0.9525 (0.9320, 0.9660)
$\gamma_6^{c,d}$	0.0002 (-0.0026, 0.0066)	0.0485 (0.0224, 0.0995)	0.0542 (0.0238, 0.1250)	0.9450 (0.9300, 0.9620)
$\gamma_7^{c,d}$	0.0011 (-0.0020, 0.0063)	0.0405 (0.0141, 0.0959)	0.0508 (0.0231, 0.1109)	0.9500 (0.9390, 0.9700)
$\gamma_8^{c,d}$	0.0012 (-0.0028, 0.0058)	0.0400 (0.0141, 0.1015)	0.0548 (0.0227, 0.1377)	0.9475 (0.9390, 0.9620)
$\gamma_9^{c,d}$	0.0014 (-0.0027, 0.0069)	0.0424 (0.0141, 0.1068)	0.0654 (0.0230, 0.2185)	0.9475 (0.9390, 0.9620)
θ_ϵ	-0.0032 (-0.0064, -0.0002)	0.0442 (0.0200, 0.1010)	0.0334 (0.0211, 0.0509)	0.9445 (0.9370, 0.9620)

^a SE: standard error.

^b RMSE: root mean square error.

^c γ_j ($j = 2, \dots, 9$) indicates the relative rate-of-change (i.e., the absolute rate of change over the shape factor) in the j^{th} time interval.

^d The summary of metrics for γ_j ($j = 6, \dots, 9$) was based on the estimates from the conditions with ten measurement occasions.

Table 6: Summary of Performance Metrics of Quadratic Latent Change Score Model and Corresponding Latent Growth Curve Model

Para.	Relative Bias	Empirical SE ^a	Relative RMSE ^b	Coverage Probability
Latent Change Score Model				
μ_{η_0}	0.0000 (−0.0001, 0.0006)	0.2955 (0.2209, 0.3726)	0.0059 (0.0044, 0.0074)	0.9480 (0.9340, 0.9580)
μ_{η_1}	0.0000 (−0.0003, 0.0003)	0.0748 (0.0480, 0.1109)	0.0040 (0.0024, 0.0069)	0.9445 (0.9370, 0.9530)
μ_{η_2}	0.0000 (−0.0008, 0.0006)	0.0198 (0.0141, 0.0265)	−0.0152 (−0.0216, −0.0099)	0.9490 (0.9370, 0.9590)
ψ_{00}	−0.0039 (−0.0091, 0.0031)	2.1461 (1.5469, 2.6927)	0.0858 (0.0619, 0.1077)	0.9410 (0.9320, 0.9610) ^c
ψ_{01}	−0.0043 (−0.0110, 0.0055)	0.3837 (0.2410, 0.5782)	0.2558 (0.1610, 0.3853)	0.9480 (0.9400, 0.9630)
ψ_{02}	−0.0060 (−0.0193, 0.0149)	0.1013 (0.0707, 0.1432)	0.2255 (0.1571, 0.3184)	0.9460 (0.9310, 0.9560)
ψ_{11}	−0.0047 (−0.0136, −0.0028)	0.1179 (0.0714, 0.2458)	0.1179 (0.0712, 0.2458)	0.9430 (0.9340, 0.9540)
ψ_{12}	−0.0043 (−0.0110, 0.0055)	0.0245 (0.0141, 0.0469)	0.2629 (0.1638, 0.5228)	0.9490 (0.9370, 0.9670)
ψ_{22}	−0.0042 (−0.0128, 0.0023)	0.0100 (0.0000, 0.0141)	0.1016 (0.0632, 0.1695)	0.9475 (0.9240, 0.9540)
θ_ϵ	0.0000 (−0.0015, 0.0022)	0.0485 (0.0245, 0.1136)	0.0369 (0.0237, 0.0579)	0.9515 (0.9420, 0.9590)
Latent Growth Curve Model				
μ_{η_0}	0.0000 (−0.0001, 0.0006)	0.2955 (0.2209, 0.3726)	0.0059 (0.0044, 0.0074)	0.9480 (0.9340, 0.9580)
μ_{η_1}	0.0000 (−0.0003, 0.0003)	0.0748 (0.0480, 0.1109)	0.0040 (0.0024, 0.0069)	0.9445 (0.9370, 0.9530)
μ_{η_2}	0.0000 (−0.0008, 0.0006)	0.0198 (0.0141, 0.0265)	−0.0152 (−0.0216, −0.0099)	0.9490 (0.9370, 0.9590)
ψ_{00}	−0.0039 (−0.0091, 0.0031)	2.1461 (1.5469, 2.6927)	0.0858 (0.0619, 0.1077)	0.9410 (0.9330, 0.9610) ^c
ψ_{01}	−0.0043 (−0.0110, 0.0055)	0.3837 (0.2410, 0.5782)	0.2558 (0.1610, 0.3853)	0.9480 (0.9400, 0.9630)
ψ_{02}	−0.0060 (−0.0193, 0.0149)	0.1013 (0.0707, 0.1432)	0.2255 (0.1571, 0.3184)	0.9460 (0.9310, 0.9560)
ψ_{11}	−0.0047 (−0.0136, −0.0028)	0.1179 (0.0714, 0.2458)	0.1179 (0.0712, 0.2458)	0.9430 (0.9340, 0.9540)
ψ_{12}	−0.0043 (−0.0110, 0.0055)	0.0245 (0.0141, 0.0469)	0.2629 (0.1638, 0.5228)	0.9490 (0.9370, 0.9670)
ψ_{22}	−0.0042 (−0.0128, 0.0023)	0.0100 (0.0000, 0.0141)	0.1016 (0.0632, 0.1695)	0.9475 (0.9240, 0.9540)
θ_ϵ	0.0000 (−0.0015, 0.0022)	0.0485 (0.0245, 0.1136)	0.0369 (0.0237, 0.0579)	0.9515 (0.9420, 0.9590)

^a SE: standard error.^b RMSE: root mean square error.^c These cells include a different summary of the performance metric of the quadratic latent change score model and that of the corresponding latent growth curve model.

Table 7: Summary of Performance Metrics of Negative Exponential Latent Change Score Model and Corresponding Latent Growth Curve Model

Para.	Relative Bias	Empirical SE ^a	Relative RMSE ^b	Coverage Probability
Latent Change Score Model				
μ_{η_0}	0.0000 (−0.0004, 0.0005)	0.2963 (0.2198, 0.3735)	0.0060 (0.0044, 0.0075)	0.9500 (0.9280, 0.9620)
μ_{η_1}	0.0130 (0.0059, 0.0296)	0.2043 (0.1382, 0.3058)	0.0159 (0.0077, 0.0307)	0.5285 (0.0000, 0.8910)
b	−0.0015 (−0.0036, 0.0005)	0.0000 (0.0000, 0.0100)	0.0069 (0.0041, 0.0177)	0.9395 (0.8610, 0.9590)
ψ_{00}	−0.0029 (−0.0076, 0.0023)	2.1559 (1.6138, 2.6852)	0.0863 (0.0645, 0.1074)	0.9435 (0.9270, 0.9540)
ψ_{01}	0.0102 (−0.0037, 0.0317)	1.0082 (0.7222, 1.3685)	0.2248 (0.1623, 0.3041)	0.9530 (0.9370, 0.9670)
ψ_{11}	0.0226 (0.0029, 0.0636)	0.9249 (0.6204, 1.3684)	0.1086 (0.0696, 0.1571)	0.9485 (0.8910, 0.9650)
θ_ϵ	0.0000 (−0.0025, 0.0013)	0.0458 (0.0224, 0.0990)	0.0336 (0.0214, 0.0506)	0.9485 (0.9360, 0.9630)
Latent Growth Curve Model				
μ_{η_0}	0.0000 (−0.0004, 0.0005)	0.2963 (0.2198, 0.3735)	0.0060 (0.0044, 0.0075)	0.9495 (0.9300, 0.9620)
μ_{η_1}	0.0000 (−0.0003, 0.0003)	0.2043 (0.1353, 0.3077)	0.0068 (0.0045, 0.0103)	0.9480 (0.9330, 0.9620)
b	0.0000 (−0.0004, 0.0005)	0.0000 (0.0000, 0.0100)	0.0063 (0.0035, 0.0177)	0.9530 (0.9240, 0.9600)
ψ_{00}	−0.0029 (−0.0076, 0.0023)	2.1559 (1.6137, 2.6853)	0.0863 (0.0645, 0.1074)	0.9435 (0.9260, 0.9540)
ψ_{01}	−0.0023 (−0.0106, 0.0041)	0.9960 (0.7010, 1.3585)	0.2212 (0.1557, 0.3017)	0.9515 (0.9370, 0.9620)
ψ_{11}	−0.0032 (−0.0093, 0.0034)	0.9125 (0.6132, 1.3484)	0.1016 (0.0681, 0.1497)	0.9435 (0.9290, 0.9610)
θ_ϵ	−0.0007 (−0.0026, 0.0013)	0.0458 (0.0224, 0.0990)	0.0335 (0.0214, 0.0507)	0.9485 (0.9370, 0.9630)

^a SE: standard error.^b RMSE: root mean square error.

Table 8: Summary of Performance Metrics of Jeness-Bayley Latent Change Score Model and Corresponding Latent Growth Curve Model

Para.	Relative Bias	Empirical SE ^a	Relative RMSE ^b	Coverage Probability
Latent Change Score Model				
μ_{η_0}	-0.0002 (-0.0004, 0.0002)	0.2919 (0.2216, 0.3686)	0.0058 (0.0044, 0.0074)	0.9495 (0.9350, 0.9580)
μ_{η_1}	-0.0021 (-0.0299, 0.0091)	0.0624 (0.0245, 0.1947)	0.0346 (0.0193, 0.1930)	0.9470 (0.9270, 0.9660)
μ_{η_2}	0.0232 (0.0125, 0.0289)	0.3126 (0.1778, 1.0191)	-0.0248 (-0.0443, -0.0138)	0.5930 (0.0180, 0.9100)
c	-0.0019 (-0.0065, 0.0002)	0.0100 (0.0000, 0.0265)	-0.0137 (-0.0384, -0.0069)	0.9435 (0.9310, 0.9590)
ψ_{00}	-0.0033 (-0.0097, 0.0012)	2.1538 (1.5806, 2.7194)	0.0864 (0.0632, 0.1091)	0.9410 (0.9260, 0.9600)
ψ_{01}	-0.0058 (-0.0168, 0.0088)	0.2474 (0.1039, 0.5098)	0.2558 (0.1631, 0.5755)	0.9500 (0.9320, 0.9610)
ψ_{02}	0.0174 (-0.0028, 0.0378)	1.2792 (0.8166, 2.0289)	0.2842 (0.1823, 0.4517)	0.9510 (0.9300, 0.9630)
ψ_{11}	-0.0052 (-0.0173, 0.0078)	0.0636 (0.0100, 0.1655)	0.1056 (0.0618, 0.5676)	0.9450 (0.9300, 0.9610)
ψ_{12}	0.0174 (-0.0115, 0.0589)	0.1885 (0.0762, 0.5652)	0.3251 (0.1876, 1.2615)	0.9485 (0.9370, 0.9620)
ψ_{22}	0.0418 (0.0199, 0.0583)	1.2261 (0.7643, 2.9078)	0.1432 (0.0876, 0.3274)	0.9500 (0.9340, 0.9620)
θ_ϵ	-0.0006 (-0.0035, 0.0024)	0.0490 (0.0224, 0.1200)	0.0372 (0.0230, 0.0600)	0.9490 (0.9370, 0.9570)
Latent Growth Curve Model				
μ_{η_0}	-0.0001 (-0.0003, 0.0002)	0.2920 (0.2216, 0.3685)	0.0058 (0.0044, 0.0074)	0.9490 (0.9360, 0.9590)
μ_{η_1}	-0.0006 (-0.0083, 0.0058)	0.0624 (0.0245, 0.1949)	0.0344 (0.0191, 0.1906)	0.9475 (0.9350, 0.9630)
μ_{η_2}	0.0002 (-0.0006, 0.0026)	0.3153 (0.1786, 1.0393)	-0.0105 (-0.0347, -0.0059)	0.9510 (0.9360, 0.9630)
c	0.0000 (-0.0010, 0.0018)	0.0100 (0.0000, 0.0265)	-0.0137 (-0.0384, -0.0070)	0.9485 (0.9310, 0.9590)
ψ_{00}	-0.0033 (-0.0097, 0.0012)	2.1537 (1.5805, 2.7190)	0.0864 (0.0632, 0.1091)	0.9410 (0.9270, 0.9600)
ψ_{01}	-0.0063 (-0.0155, 0.0070)	0.2475 (0.1039, 0.5085)	0.2558 (0.1630, 0.5731)	0.9495 (0.9330, 0.9630)
ψ_{02}	-0.0053 (-0.0176, 0.0139)	1.2597 (0.7977, 1.9744)	0.2799 (0.1772, 0.4386)	0.9480 (0.9220, 0.9630)
ψ_{11}	-0.0053 (-0.0215, 0.0064)	0.0636 (0.0141, 0.1649)	0.1056 (0.0618, 0.5632)	0.9445 (0.9300, 0.9630)
ψ_{12}	-0.0054 (-0.0409, 0.0154)	0.1853 (0.0748, 0.5498)	0.3200 (0.1840, 1.2216)	0.9460 (0.9310, 0.9570)
ψ_{22}	-0.0036 (-0.0130, 0.0037)	1.1681 (0.7294, 2.7687)	0.1298 (0.0814, 0.3075)	0.9445 (0.9320, 0.9530)
θ_ϵ	-0.0009 (-0.0045, 0.0018)	0.0490 (0.0224, 0.1200)	0.0372 (0.0230, 0.0600)	0.9475 (0.9350, 0.9600)

^a SE: standard error.

^b RMSE: root mean square error.

Table 9: Mean and Standard Deviation of Reading IRT Scores for the ECLS-K: 2011 Analytic Sample

Grade	Semester	Mean (SD) of Observed Scores	Mean (SD) of Observed Change-from-baseline
Kindergarten	Fall	54.63 (12.56)	—
	Spring	69.10 (15.33)	14.47 (8.56)
First grade	Fall	78.24 (17.57)	23.61 (11.21)
	Spring	95.85 (17.70)	41.23 (13.48)
Second grade	Fall	102.04 (17.60)	47.41 (13.73)
	Spring	112.52 (17.08)	57.90 (13.73)
Third grade	Spring	120.56 (15.06)	65.93 (13.40)
Fourth grade	Spring	129.18 (14.63)	74.55 (12.63)
Fifth grade	Spring	135.94 (14.89)	81.31 (13.90)

Note: IRT = item response theory; ECLS-K: 2011 = Early Childhood Longitudinal Study, Kindergarten Class 2010-11; SD = standard deviation.

Table 10: Summary of Model Fit Information For the Models

Model	-2ll	AIC	BIC	# of Para.	Residual
Latent Basis Growth Model	26205.17	26232.11	26241.81	13	49.208
Quadratic Latent Change Score Model	26527.88	26548.45	26556.07	10	48.753
Negative Exponential Latent Change Score Model	26617.17	26631.46	26636.90	7	53.997
Jeness-Bayley Latent Change Score Model	26392.76	26415.44	26423.76	11	45.749
Quadratic Latent Growth Curve Model	26464.57	26485.14	26492.76	10	48.933
Negative Exponential Latent Growth Curve Model	26609.86	26624.14	26629.59	7	54.015
Jeness-Bayley Latent Growth Curve Model	26362.91	26385.59	26393.91	11	46.120

Table 11: Estimates of Nonparametric Latent Change Score Model

Para.	Estimate (SE)	P value	Para.	Estimate (SE)	P value	Para.	Estimate (SE)	P value
μ_{η_0}	54.724 (0.804)	< 0.0001 ^a						
μ_{η_1}	29.401 (1.015)	< 0.0001*						
ψ_{00}	210.702 (16.402)	< 0.0001*						
ψ_{01}	-22.422 (4.309)	< 0.0001*						
ψ_{11}	19.562 (2.262)	< 0.0001*						
θ_ϵ	49.208 (1.315)	< 0.0001*						
γ_1^b	1.000 (0.000)	—	$\mu_{d_1}^c$	29.401 (1.015)	< 0.0001*	$\phi_{d_1}^d$	19.562 (2.272)	< 0.0001*
γ_2^b	0.641 (0.047)	< 0.0001*	$\mu_{d_2}^c$	18.851 (0.962)	< 0.0001*	$\phi_{d_2}^d$	8.042 (1.115)	< 0.0001*
γ_3^b	1.159 (0.051)	< 0.0001*	$\mu_{d_3}^c$	34.074 (0.962)	< 0.0001*	$\phi_{d_3}^d$	26.276 (2.935)	< 0.0001*
γ_4^b	0.472 (0.037)	< 0.0001*	$\mu_{d_4}^c$	13.882 (0.995)	< 0.0001*	$\phi_{d_4}^d$	4.361 (0.742)	< 0.0001*
γ_5^b	0.660 (0.038)	< 0.0001*	$\mu_{d_5}^c$	19.416 (0.917)	< 0.0001*	$\phi_{d_5}^d$	8.532 (1.152)	< 0.0001*
γ_6^b	0.286 (0.020)	< 0.0001*	$\mu_{d_6}^c$	8.411 (0.506)	< 0.0001*	$\phi_{d_6}^d$	1.601 (0.243)	< 0.0001*
γ_7^b	0.283 (0.019)	< 0.0001*	$\mu_{d_7}^c$	8.325 (0.490)	< 0.0001*	$\phi_{d_7}^d$	1.568 (0.236)	< 0.0001*
γ_8^b	0.231 (0.018)	< 0.0001*	$\mu_{d_8}^c$	6.796 (0.491)	< 0.0001*	$\phi_{d_8}^d$	1.045 (0.180)	< 0.0001*

^a * indicates statistical significance at 0.05 level.

^b $\gamma_1 = 1$, which is fixed in our model specification. γ_j ($j = 2, \dots, 8$) indicates the relative rate-of-change (i.e., the absolute rate of change over the shape factor) in the j^{th} time interval.

^c $\mu_{d_j} = \mu_{\eta_1} \gamma_j$ ($j = 1, \dots, 8$) indicates the estimated mean value of the absolute rate-of-change in the j^{th} time interval.

^d $\phi_{d_j, \text{mid}}$ ($j = 1, \dots, 8$) indicates the estimated variance of the absolute rate-of-change the j^{th} interval.

Table 12: Estimates of Quadratic Latent Change Score Model

Para.	Estimate (SE)	P value	Para.	Estimate (SE)	P value	Para.	Estimate (SE)	P value
μ_{η_0}	55.883 (0.713)	< 0.0001 ^a	$\mu_{d_{1, \text{mid}}}^b$	26.871 (0.360)	< 0.0001*	$\phi_{d_{1, \text{mid}}}^c$	32.092 (3.750)	< 0.0001*
μ_{η_1}	31.023 (0.455)	< 0.0001*	$\mu_{d_{2, \text{mid}}}^b$	24.444 (0.306)	< 0.0001*	$\phi_{d_{2, \text{mid}}}^c$	24.021 (2.719)	< 0.0001*
μ_{η_2}	-2.489 (0.062)	< 0.0001*	$\mu_{d_{3, \text{mid}}}^b$	21.942 (0.253)	< 0.0001*	$\phi_{d_{3, \text{mid}}}^c$	17.285 (1.871)	< 0.0001*
ψ_{00}	175.965 (14.393)	< 0.0001*	$\mu_{d_{4, \text{mid}}}^b$	19.478 (0.206)	< 0.0001*	$\phi_{d_{4, \text{mid}}}^c$	12.217 (1.246)	< 0.0001*
ψ_{01}	9.258 (7.306)	0.2050	$\mu_{d_{5, \text{mid}}}^b$	16.968 (0.168)	< 0.0001*	$\phi_{d_{5, \text{mid}}}^c$	8.655 (0.825)	< 0.0001*
ψ_{02}	-2.860 (0.965)	0.0031*	$\mu_{d_{6, \text{mid}}}^b$	13.246 (0.147)	< 0.0001*	$\phi_{d_{6, \text{mid}}}^c$	6.343 (0.608)	< 0.0001*
ψ_{11}	49.393 (5.992)	< 0.0001*	$\mu_{d_{7, \text{mid}}}^b$	8.355 (0.196)	< 0.0001*	$\phi_{d_{7, \text{mid}}}^c$	8.703 (1.081)	< 0.0001*
ψ_{12}	-5.848 (0.780)	< 0.0001*	$\mu_{d_{8, \text{mid}}}^b$	3.378 (0.293)	< 0.0001*	$\phi_{d_{8, \text{mid}}}^c$	17.399 (2.415)	< 0.0001*
ψ_{22}	0.794 (0.108)	< 0.0001*						
θ_ϵ	48.753 (1.413)	< 0.0001*						

^a * indicates statistical significance at 0.05 level.

^b $\mu_{d_{j, \text{mid}}}$ ($j = 1, \dots, 8$) indicates the estimated mean value of the instantaneous slope midway the j^{th} interval.

^c $\phi_{d_{j, \text{mid}}}$ ($j = 1, \dots, 8$) indicates the estimated variance of the instantaneous slope midway the j^{th} interval.

Table 13: Estimates of Negative Exponential Latent Change Score Model

Para.	Estimate (SE)	P value	Para.	Estimate (SE)	P value	Para.	Estimate (SE)	P value
μ_{η_0}	54.417 (0.785)	< 0.0001 ^a	$\mu_{d_{1_mid}}$ ^b	30.669 (0.450)	< 0.0001*	$\phi_{d_{1_mid}}$ ^c	28.748 (2.890)	< 0.0001*
μ_{η_1}	118.531 (1.211)	< 0.0001*	$\mu_{d_{2_mid}}$ ^b	25.919 (0.326)	< 0.0001*	$\phi_{d_{2_mid}}$ ^c	20.533 (2.019)	< 0.0001*
ψ_{00}	209.538 (16.562)	< 0.0001*	$\mu_{d_{3_mid}}$ ^b	21.794 (0.238)	< 0.0001*	$\phi_{d_{3_mid}}$ ^c	14.517 (1.401)	< 0.0001*
ψ_{01}	-47.027 (18.854)	0.0126*	$\mu_{d_{4_mid}}$ ^b	18.372 (0.184)	< 0.0001*	$\phi_{d_{4_mid}}$ ^c	10.317 (0.980)	< 0.0001*
ψ_{11}	429.413 (40.461)	< 0.0001*	$\mu_{d_{5_mid}}$ ^b	15.440 (0.156)	< 0.0001*	$\phi_{d_{5_mid}}$ ^c	7.286 (0.684)	< 0.0001*
γ	0.345 (0.006)	< 0.0001*	$\mu_{d_{6_mid}}$ ^b	11.929 (0.143)	< 0.0001*	$\phi_{d_{6_mid}}$ ^c	4.349 (0.405)	< 0.0001*
θ_ϵ	53.997 (1.452)	< 0.0001*	$\mu_{d_{7_mid}}$ ^b	8.500 (0.138)	< 0.0001*	$\phi_{d_{7_mid}}$ ^c	2.208 (0.207)	< 0.0001*
			$\mu_{d_{8_mid}}$ ^b	6.020 (0.130)	< 0.0001*	$\phi_{d_{8_mid}}$ ^c	1.108 (0.106)	< 0.0001*

^a * indicates statistical significance at 0.05 level.

^b $\mu_{d_{j_mid}}$ ($j = 1, \dots, 8$) indicates the estimated mean value of the instantaneous slope midway the j^{th} interval.

^c $\phi_{d_{j_mid}}$ ($j = 1, \dots, 8$) indicates the estimated variance of the instantaneous slope midway the j^{th} interval.

Table 14: Estimates of Jeness-Bayley Latent Change Score Model

Para.	Estimate (SE)	P value	Para.	Estimate (SE)	P value	Para.	Estimate (SE)	P value
μ_{η_0}	54.340 (0.707)	< 0.0001 ^a	$\mu_{d_{1_mid}}$ ^b	30.775 (0.571)	< 0.0001*	$\phi_{d_{1_mid}}$ ^c	58.575 (7.023)	< 0.0001*
μ_{η_1}	-1.458 (1.278)	0.2541	$\mu_{d_{2_mid}}$ ^b	26.138 (0.379)	< 0.0001*	$\phi_{d_{1_mid}}$ ^c	35.740 (3.953)	< 0.0001*
μ_{η_2}	-131.988 (11.755)	< 0.0001*	$\mu_{d_{3_mid}}$ ^b	22.056 (0.270)	< 0.0001*	$\phi_{d_{1_mid}}$ ^c	21.016 (2.153)	< 0.0001*
ψ_{00}	167.39 (13.886)	< 0.0001*	$\mu_{d_{4_mid}}$ ^b	18.626 (0.220)	< 0.0001*	$\phi_{d_{1_mid}}$ ^c	12.531 (1.202)	< 0.0001*
ψ_{01}	-32.172 (5.716)	< 0.0001*	$\mu_{d_{5_mid}}$ ^b	15.647 (0.193)	< 0.0001*	$\phi_{d_{1_mid}}$ ^c	8.045 (0.736)	< 0.0001*
ψ_{02}	-186.537 (48.621)	0.0001*	$\mu_{d_{6_mid}}$ ^b	12.022 (0.168)	< 0.0001*	$\phi_{d_{1_mid}}$ ^c	6.201 (0.618)	< 0.0001*
ψ_{11}	34.157 (6.445)	< 0.0001*	$\mu_{d_{7_mid}}$ ^b	8.400 (0.189)	< 0.0001*	$\phi_{d_{1_mid}}$ ^c	8.321 (1.012)	< 0.0001*
ψ_{12}	271.19 (56.553)	< 0.0001*	$\mu_{d_{8_mid}}$ ^b	5.711 (0.291)	< 0.0001*	$\phi_{d_{1_mid}}$ ^c	12.458 (1.644)	< 0.0001*
ψ_{22}	2630.396 (516.047)	< 0.0001*						
γ	-0.318 (0.025)	< 0.0001*						
θ_ϵ	45.749 (1.327)	< 0.0001*						

^a * indicates statistical significance at 0.05 level.

^b $\mu_{d_{j_mid}}$ ($j = 1, \dots, 8$) indicates the estimated mean value of the instantaneous slope midway the j^{th} interval.

^c $\phi_{d_{j_mid}}$ ($j = 1, \dots, 8$) indicates the estimated variance of the instantaneous slope midway the j^{th} interval.